



The FOXP2-Driven Network in Developmental Disorders and Neurodegeneration

Franz Oswald^{1†}, Patricia Klöble^{1†}, André Ruland¹, David Rosenkranz², Bastian Hinz^{2,3}, Falk Butter⁴, Sanja Ramljak⁵, Ulrich Zechner^{3,6‡} and Holger Herlyn^{2*†}

¹ Center for Internal Medicine, Department of Internal Medicine I, University Medical Center Ulm, Ulm, Germany, ² Institut für Organismische und Molekulare Evolutionsbiologie, Johannes Gutenberg-University Mainz, Mainz, Germany, ³ Institute of Human Genetics, University Medical Center Mainz, Mainz, Germany, ⁴ Institute of Molecular Biology, Mainz, Germany, ⁵ Sciema UG, Mainz, Germany, ⁶ Dr. Senckenbergisches Zentrum für Humangenetik, Frankfurt, Germany

OPEN ACCESS

Edited by:

Jaewon Ko,
Daegu Gyeongbuk Institute
of Science and Technology (DGIST),
South Korea

Reviewed by:

Cedric Boeckx,
Institutió Catalana de Recerca i
Estudis Avançats (ICREA), Spain
Kihoon Han,
Korea University College of Medicine,
South Korea

*Correspondence:

Holger Herlyn
herlyn@uni-mainz.de

[†]Shared first authorship

[‡]Shared senior authorship

Received: 24 March 2017

Accepted: 04 July 2017

Published: 26 July 2017

Citation:

Oswald F, Klöble P, Ruland A,
Rosenkranz D, Hinz B, Butter F,
Ramljak S, Zechner U and Herlyn H
(2017) The FOXP2-Driven Network
in Developmental Disorders
and Neurodegeneration.
Front. Cell. Neurosci. 11:212.
doi: 10.3389/fncel.2017.00212

The transcription repressor FOXP2 is a crucial player in nervous system evolution and development of humans and songbirds. In order to provide an additional insight into its functional role we compared target gene expression levels between human neuroblastoma cells (SH-SY5Y) stably overexpressing FOXP2 cDNA of either humans or the common chimpanzee, Rhesus monkey, and marmoset, respectively. RNA-seq led to identification of 27 genes with differential regulation under the control of human FOXP2, which were previously reported to have FOXP2-driven and/or songbird song-related expression regulation. RT-qPCR and Western blotting indicated differential regulation of additional 13 new target genes in response to overexpression of human FOXP2. These genes may be directly regulated by FOXP2 considering numerous matches of established FOXP2-binding motifs as well as publicly available FOXP2-ChIP-seq reads within their putative promoters. Ontology analysis of the new and reproduced targets, along with their interactors in a network, revealed an enrichment of terms relating to cellular signaling and communication, metabolism and catabolism, cellular migration and differentiation, and expression regulation. Notably, terms including the words “neuron” or “axonogenesis” were also enriched. Complementary literature screening uncovered many connections to human developmental (autism spectrum disease, schizophrenia, Down syndrome, agenesis of corpus callosum, trismus-pseudocamptodactyly, ankyloglossia, facial dysmorphology) and neurodegenerative diseases and disorders (Alzheimer’s, Parkinson’s, and Huntington’s diseases, Lewy body dementia, amyotrophic lateral sclerosis). Links to deafness and dyslexia were detected, too. Such relations existed for single proteins (e.g., DCDC2, NURR1, PHOX2B, MYH8, and MYH13) and groups of proteins which conjointly function in mRNA processing, ribosomal recruitment, cell–cell adhesion (e.g., CDH4), cytoskeleton organization, neuro-inflammation, and processing of amyloid precursor protein. Conspicuously, many links pointed to an involvement of the FOXP2-driven network in JAK/STAT signaling and the regulation of the ezrin–radixin–moesin complex. Altogether, the applied phylogenetic perspective substantiated FOXP2’s

importance for nervous system development, maintenance, and functioning. However, the study also disclosed new regulatory pathways that might prove to be useful for understanding the molecular background of the aforementioned developmental disorders and neurodegenerative diseases.

Keywords: language, speech, brain, schizophrenia, Parkinson's disease, Alzheimer's disease, Huntington's disease, neuronal circuitry

INTRODUCTION

The high complexity clearly sets apart human verbal communication from vocalization repertoires of other primate species. Yet, despite this importance we are still at the beginning of understanding the molecular pathways behind the evolutionary and developmental acquisition of speech and language. Probably, the most advancement was made in respect to the role of the gene coding for forkhead box P2 (FOXP2; O15409; also CAGH44). The encoded transcription repressor spans 715 amino acids (aa) in human isoform I, thereby containing the eponymous forkhead box domain with DNA-binding ability at the C-terminus, a central expression suppression domain with zinc finger and leucine zipper motifs, and a glutamine-enriched N-terminus, with the longest poly-glutamine stretch spanning 40 aa (**Figure 1A**; e.g., Vernes and Fisher, 2009; Enard, 2011).

FOXP2's relevance for verbal communication became obvious when a missense mutation in the coding gene (p.R553H) which lowers the DNA binding capability was recognized to associate with speech-language disorder 1 (SPCH1, OMIM #602081), also known as developmental verbal dyspraxia (DVD) and childhood apraxia of speech (CAS). Affected family members suffered from deficits in virtually every aspect of expressive and receptive language. They especially showed disturbed orofacial motor coordination affecting tongue, lips, jaw and palate, which together led to impaired lingual articulation and non-lingual sound-production (e.g., Vernes and Fisher, 2009). The subsequent recognition of associations between other FOXP2 mutations and communication disorders further substantiated the importance of the gene for the acquisition of full speech and language competence (Vernes and Fisher, 2009; Palka et al., 2012). FOXP2 has additionally been implicated in the etiology of mental diseases such as autism spectrum disorder (ASD; Bowers and Konopka, 2012) and schizophrenia (SCZD; e.g., Jamadar et al., 2011; Li et al., 2013). Notably, also these disorders are frequently accompanied by language and speech deficits (e.g., Stephane et al., 2007; Abrahams and Geschwind, 2010; Kupferberg, 2010) so that studies on FOXP2 hold out the prospect of elucidating the evolution and development of speech and language (e.g., Marcus and Fisher, 2003; Bolhuis et al., 2010; Enard, 2011).

The FOXP2 gene is expressed in multiple tissues including fetal and adult brain (e.g., Vernes and Fisher, 2009; Enard, 2011) whereby haploinsufficiency and thus lowered levels of transcript and protein are commonly assumed to elicit the aforementioned diseases and disorders (e.g., Enard, 2011). In support of this view,

all documented patients were heterozygous for the etiological mutation (Vernes and Fisher, 2009) in either the gene itself (point mutations, deletions, chromosomal rearrangements; e.g., Turner et al., 2013 and references therein) or downstream regulatory elements (e.g., Adegbola et al., 2015). Random mono-allelic expression (RMAE) with some cells having half the FOXP2 dosage and others expressing none at all (Adegbola et al., 2015) and mosaic deletion with some cells possessing two functional alleles and others none (Palka et al., 2012) also play a role. Either way, minimum expression of one functional allele in at least part of the cells seems indispensable to life, a condition that is additionally demonstrated by early post-natal death of mice homozygous for a *Foxp2* null allele (French et al., 2007; Vernes et al., 2007; Rousso et al., 2012).

FOXP2's influence on human vocalization skills has a stunning parallel in non-primate vocal-learners. In songbirds, brain FOXP2 levels positively associate with vocal learning and singing activity whereas knockdown impairs song learning (see, e.g., Bolhuis et al., 2010; Pfenning et al., 2014). In line with this, FOXP2 belonged to the highly supported genes in a genome-wide screen for singing-related transcriptional changes in male zebra finch brains (see Hilliard et al., 2012). Investigation of other bird and additional mammalian species underlined a general pattern confirming that normal development of vocal learning and vocalization skills requires fine-tuned regulation of FOXP2 expression in brain (e.g., Bolhuis et al., 2010; Pfenning et al., 2014).

The human–bird parallel demonstrates that FOXP2's origin predates the split of Mammalia and Sauropsida about 320 million years ago (timetree.org estimate). Yet, regardless of hundreds of millions of years of independent evolution zebra finch FOXP2 still shows 98% identity with the human ortholog (Haesler et al., 2004). Evolutionary conservation of FOXP2 also prevailed throughout the divergence of primates, though with a notable exception: Thus, two aa substitutions, p.T303N and p.N325S (rs753394697 SNP), occurred on the human branch after the split from the chimpanzee lineage. These two exchanges reside inside the transcription repression domain (**Figure 1A**) and potentially were exposed to positive selection (reviewed in Enard, 2011; also, e.g., Mozzi et al., 2016). However, according to genome-wide evidence the selective sweep was not complete (Mallick et al., 2016) so that FOXP2 evolution in primates and especially in humans was probably more complex than previously thought. In any case, the two aa exchanges known from humans seem to be functional. Thus, mice homozygous for a *Foxp2* version mutated for both human exchanges had reduced dopamine concentration in all investigated brain regions and their striatal medium spiny neurons showed

SH-SY5Y cells overexpressing either human *FOXP2* cDNA or a variant in which both human-specific non-synonymous substitutions were mutated to acquire the chimpanzee-specific aa content at the respective sites (*FOXP2*^{chimp} in Konopka et al., 2009). The latter study as well as additional ones with a focus on the effect of both human-specific aa substitutions in mutated mice (*Foxp2*^{hum} in Enard et al., 2009 and follow-up studies) generated valuable data on FOXP2/*Foxp2* functioning. However, the interpretability of the data is fairly challenging from an evolutionary point of view, due to the following: Understanding the evolutionary meaning behind differential target gene expression levels in a pair of models representing two extant species requires considerable assumptions in regard to expression levels in an unknown ancestor. Without such assumptions it is not possible to certainly assign an evolutionary change to either one or the other lineage. Neither parental cells nor cells carrying empty vector can appropriately model the ancestral condition as they rather reflect baseline expression levels in extant species as do wild-type animals in respective comparisons. Moreover, the mutated *FOXP2/Foxp2* variants which merge states of two species in a single cDNA (*FOXP2*^{chimp}, *Foxp2*^{hum}) have no counterparts in living species and it is questionable if they have ever existed in any human ancestor. This is due to additional synonymous (silent) and non-synonymous nucleotide substitutions in the human–mouse and human–chimpanzee comparison (see, e.g., Enard et al., 2002). Variant lengths of the CAG/CAA repeats coding for the N-terminal FOXP2 poly-glutamine tracts additionally contribute to this discrepancy (Figure 1A). Yet, the outlined restraints in terms of evolutionary interpretability can be overcome in a broader phylogenetic context which addresses the effect of human *FOXP2* relative to naturally occurring cDNAs of chimpanzee and at least one further non-human species. In such a phylogenetic approach unidirectional differences in target gene expression levels between the human model on the one hand and the non-human models on the other give an approximation of potential expressional changes in human evolution.

Synonymous exchanges might indeed have functional relevance on FOXP2 expression, namely through nucleotide (Debatisse et al., 2004) and tRNA availability (Wohlgemuth et al., 2013). It is also conceivable that extension of the longest of N-terminal poly-glutamine tracts is functionally relevant. The respective stretch spans 40 aa in the human reference (*Homo sapiens* FOXP2, hsaFOXP2) whereas it has 41, 39, and 38 glutamines in the FOXP2 of common chimpanzee (*Pan troglodytes*, ptrFOXP2), Rhesus monkey (*Macaca mulatta*, mmuFOXP2), and white-tufted ear marmoset (*Callithrix jacchus*, cjaFOXP2), respectively (Figure 1B). Although these interspecific differences may appear negligible they seem to evolve under functional constraint as suggested by a general tendency of repeat length conservation in humans (Bruce and Margolis, 2002). In support of this view, mutations decreasing the number of N-terminal glutamines in FOXP2 were found to occur in speech and sound disorder (SSD) patients. Also, the fact that a deletion of glutamines from the FOXP2 N-terminus alters expression of the language

gene *CNTNAP2* suggests that the extension of the respective stretches is functionally relevant (Zhao et al., 2015; for language association, see Abrahams and Geschwind, 2010; Kato et al., 2014). Functional relevance of poly-glutamine tract extension could be anticipated given that poly-glutamine tract expansion in other genes account for several diseases (e.g., Fan et al., 2014). On that premise, some of FOXP2's functional implications in human evolution and development might still await their discovery.

The present study investigates FOXP2's role by adopting a broader phylogenetic perspective. To the best of our knowledge, this approach takes into account for the first time the entire spectrum of differences that distinguish human *FOXP2* gene from its non-human primate counterparts. In detail, we compared expression levels between SH-SY5Y cells stably overexpressing hsaFOXP2 with corresponding levels in cells that were alternatively transfected with ptrFOXP2, mmuFOXP2, and cjaFOXP2. The species sample behind covers the major lineages inside extant anthropoid primates (New World monkeys, Old World monkeys, and Hominoidea) and at the same time allows for the identification of changes on the human branch (for phylogenetic relationships, see Figure 1B). We investigated which of the genes with specific expression regulation under hsaFOXP2 control already showed FOXP2/*Foxp2*-driven and/or songbird song-related expression regulation in previous studies. Additional attention was paid to the question if the FOXP2-driven network might be more comprehensive than known so far. We finally addressed which of the functional implications of the proteins in our network confirm previous knowledge, and which pathways might have been not observed before.

MATERIALS AND METHODS

Cell Culture and Transfection

We evaluated pcDNA3-constructs in HEK293 human embryonic kidney cells (ATCC no. CRL-1573) that were cultivated in DMEM (Gibco) supplemented with 10% FCS (Biocrom) and 1% Penicillin–Streptomycin (Gibco) at 37°C and 5% CO₂. After RT-PCR detected only minimum amount of endogenous *FOXP2* transcript (Supplementary Image 1), cells (1×10^6 cells, seeded in 8 cm dishes) were transiently transfected with Nanofectin (PAA) with 8 µg of either empty pcDNA3 expression vector (Thermo Fisher) or constructs carrying alternative primate *FOXP2* cDNAs. The custom-synthesized (BlueHeron) cDNAs used for transfection were species-specific and coded for human FOXP2 isoform I (715 aa; ENST00000350908; *Homo sapiens*, hsa) and FOXP2s in common chimpanzee (AY064549; *Pan troglodytes*, ptr), Rhesus monkey (ENSMMUT00000011202; *Macaca mulatta*, mmu), and white-tufted ear marmoset (XM_002751707; *Callithrix jacchus*, cja). Full-length transcription and translation of hsaFOXP2, ptrFOXP2, mmuFOXP2, and cjaFOXP2 was verified through specific molecular weights (plus/minus FLAG tag: higher/lower molecular weight) in Western blots 24 h after transfection (Supplementary Image 2). For the subsequent generation of

stable transfectants we used *FOXP2*-specific expression plasmids without N-terminal FLAG tag.

Parental SH-SY5Y neuroblastoma cells (ATCC no. CRL-2266) were grown in DMEM containing 15% FCS and 1% Penicillin–Streptomycin. After RT-PCR (Supplementary Image 1) detected no endogenous *FOXP2* transcript, SH-SY5Y cells were transfected with 2 μ g of either linearized empty plasmid (pcDNA3) or *FOXP2*-specific pcDNA3-constructs (see above), using the Amaxa Cell Line Nucleofector V Kit (Lonza) according to the manufacturer's instructions. This was done three times, thus generating three biological replicates per condition (designated I-III). Cells were cultivated in selection medium supplemented with 600 μ g/ml geneticin (G-418; PAA; optimized concentration according to toxicity testing) to enforce stable transfection. Stable expression of FOXP2 protein was repeatedly monitored by Western blotting (see: Immunoblotting). Efficiency and persistence of transfection were additionally monitored in SH-SY5Y cells carrying pcDNA3-eGFP constructs, by fluorescence microscopy and through Western blotting using anti-eGFP (mouse monoclonal IgG, cat 11814460001, Roche; peroxidase conjugated sheep anti-mouse IgG, NA931V, GE Healthcare).

RT-PCR and Sanger Sequencing

Coding DNAs were generated with SuperScript II (Invitrogen; random primers) from total RNAs extracted with RNeasy Mini Kit (Qiagen). Subsequent standard PCR (Taq DNA Polymerase; Invitrogen) used primers hybridizing to evolutionary conserved sites of *FOXP2* cDNA (forward: 5'-AACAGAGACCACTGCAGGTGCC-3'; reverse: 5'-TCCCTGACGCTGAAGGCTGAG-3'). For assessing levels of endogenous *FOXP2* transcription in parental HEK293 and SH-SY5Y cell lines, PCR reactions were separated on an ethidium bromide-stained agarose gel, documented under UV light, and evaluated by eye. For validating transfection of SH-SY5Y cells with the intended pcDNA3 construct, RT-PCR set the start for subsequent gel extraction of *FOXP2* bands (Gel Extraction Kit, Qiagen), ligation into TOPO vector (TOPO TA, Invitrogen), cloning into *Escherichia coli* XL1-Blue (Stratagene), plasmid preparation (Wizard Plus, Promega), and Sanger sequencing with vector primer M13 (Sequserve).

RNA Sequencing

Barcoded mRNA-seq cDNA libraries were prepared from 600 ng of total RNA of biological replicates I and II per each condition, using Illumina's TruSeq RNA Sample Preparation Kit. mRNA was isolated using oligo(d)T magnetic beads. Isolated mRNA was fragmented using divalent cations and heat and converted into cDNA using random primers and SuperScript II, followed by second strand synthesis. cDNA was end repaired, 3' adenylated and single T-overhang Illumina multiplex specific adapters were ligated to the cDNA fragments, followed by an enrichment PCR. All cleanups were done using Agencourt AMPure XP magnetic beads. The quantity of the resulting cDNA mRNA-Seq libraries was measured using Qubit. Barcoded mRNA-Seq libraries were clustered on the cBot using the TruSeq PE cluster kit V3 (10 pM) and 2 \times 50 bp were sequenced on

the Illumina HiSeq 2500 (TruSeq SBS V3 kit; 50 cycles). Raw and processed data of RNA-seq have been deposited at NCBI's Gene Expression Omnibus (GEO) under accession number GSE100291.

The raw output data of the HiSeq was preprocessed according to the Illumina standard protocol. This includes filtering for low quality reads and demultiplexing. Sequence reads were aligned to the reference genomic sequence (hg19) using STAR¹. The alignment coordinates were compared to the exon coordinates of the UCSC transcripts² and for each transcript the counts of overlapping alignments were recorded. The read counts were normalized to numbers of bases which map per kb of exon model per million mapped bases (BPKM; see Mortazavi et al., 2008) for each transcript. Comparisons between alternatively transfected cells were conducted on the basis of BPKM values as averaged over the transcripts identified.

Reverse Transcription Quantitative PCR

Coding DNA was synthesized from 2 μ g total RNA of biological replicates I and II (per each condition) by reverse transcription using oligo(d)T and random primers with SuperScript III (Invitrogen) according to the manufacturer's instructions. The cDNA samples were diluted 1:40, and 7.5 μ l of the diluted cDNA was used for reverse transcription quantitative PCR (RT-qPCR) of the candidate genes (for primers, see Supplementary Table 1.2) with QuantiTect SYBR Green Master Mix (Qiagen) on a StepOnePlus Real-Time PCR System (Life Technologies). Data was first explored with LinRegPCR³ for calculating PCR efficiency. Subsequently, relative expression was calculated using the $2^{-2\Delta\Delta C_t}$ method (Livak and Schmittgen, 2001). Measurements were carried out thrice per biological replicate. For data normalization, we measured mRNA levels of the reference genes *GAPDH* and *RPLP* (for primers, see Supplementary Table 1.2).

Immunoblotting

We focused on proteins for which commercially available antibodies yielded specific bands of the expected molecular weight in Western blots. These analyses were carried out on the basis of all three biological replicates that we prepared per condition (I-III). Protein isolation, protein quantification, SDS-PAGE, Western blotting (PVDF, Millipore), blocking and incubation with antibodies, and Enhanced Chemiluminescence (ECL, GE Healthcare) followed standard protocols. FOXP2 protein expression in transiently transfected HEK293 cells was monitored by ECL in Western blots (primary antibody: anti FOXP2 polyclonal goat anti-human, ab1307, Abcam; secondary antibody: peroxidase-conjugated rabbit anti-goat IgG, Jackson ImmunoResearch). Protein levels in stably transfected SH-SY5Y cells (all without FLAG tag) were assessed by Western blotting and ECL using the following antibodies: anti-FOXP2 (monoclonal rabbit anti-human IgG, F9050-02C, Biomol,

¹<https://github.com/alexdobin/STAR/releases>

²<https://genome.ucsc.edu/>

³www.hartfaalcentrum.nl

secondary antibody: peroxidase-conjugated donkey anti-rabbit IgG, NA934V, GE Healthcare), anti-BACE2 (mouse monoclonal IgG, sc271286, Santa Cruz Biotechnology, secondary antibody: peroxidase-conjugated sheep anti-mouse IgG, NA931V, GE Healthcare), anti-MSN (monoclonal rabbit IgG, ab52490, Abcam, secondary antibody: NA934V, GE Healthcare), anti-CDH4 (polyclonal rabbit IgG, sc7941, Santa Cruz Biotechnology, secondary antibody: NA934V, GE Healthcare). The anti-human FOXP2 antibody was raised against a peptide sequence which is conserved across the species included. Beta-actin (β -actin) served as a standard for protein loading (anti- β -actin antibody: mouse monoclonal IgG, A1978, Sigma, secondary antibody: NA931V). For densitometric analysis, signal intensity was scanned at least twice (two technical replicates) from Western blots of three biological replicates using the ImageJ software⁴.

Bioinformatics and Statistics

Gene and protein symbols accord to the recommendations of the Human Gene Nomenclature Committee.

Branch-specific synonymous (silent) and aa altering exchanges in *FOXP2* were inferred by Codeml, as implemented in the PAML package v. 4.7 (Yang, 2007). For meeting the demands of PAML, we compiled a species tree with three equally ranking branches leading to the zebra finch (*Taeniopygia guttata*), the European house mouse (*Mus musculus*), and the four primate species considered (Anthropoidea). The relationships amongst the four anthropoid species reflected the commonly accepted phylogeny (e.g., Perelman et al., 2011). Codeml analysis additionally used an alignment (ClustalX implemented in BioEdit; Hall, 1999) of the corresponding four anthropoid cDNAs (for accession numbers, see above) and of their murine (ENSMUST00000115477.7) and zebra finch (AY549148.1) orthologs.

We screened BPKM values from RNA-seq for genes whose expression levels differed in the same direction (up/down) between each of the hsaFOXP2-overexpressing SH-SY5Y transfectants and every transfectant overexpressing a non-human primate *FOXP2* cDNA or carrying empty vector. This entry criterion was tightened for new FOXP2 targets which additionally had to show at least twofold differential expression levels between the human and every other tested condition (mean *versus* mean). Statistical significance of expression levels in hsaFOXP2-overexpressing *versus* non-human primate *FOXP2*-overexpressing cells was then assessed employing the two-tailed *t*-test in SPSS v. 23.0 (IMB). The same test was applied to relative expression levels (RT-qPCR) and densitometric values (Western blotting).

Expression analyses included an evaluation of the magnitude of the effect, which stable overexpression of hsaFOXP2 had on target gene transcription and translation in SH-SY5Y cells relative to the alternative treatment with non-human primate *FOXP2* cDNAs. In detail, we calculated the correlation coefficient *r*, thereby taking into account inhomogeneous variances between samples and unequal sample sizes (Cohen, 1988). The *r*-values

were also used for *post hoc* analyses of the power of *t*-tests, which were carried out with the aid of G*Power 3.1.9.2 (Faul et al., 2009). Following the convention, we regarded *r*-values of at least 0.5 and power estimates of >80% as approximate benchmarks of large effect size and acceptable test power, respectively (Cohen, 1988).

As detailed in the legend of present Supplementary Table 2.1, we matched our RNA-seq data with previously published lists of potential targets of human FOXP2 and murine *Foxp2* as identified by Spiteri et al. (2007, their Table 1), Vernes et al. (2007, their Table 1), Enard et al. (2009, their Figures S8A,B, right panel), Konopka et al. (2009, their Supplementary Table 1), and Vernes et al. (2011, their Table S1). We additionally checked our data for matches with genes that showed singing-related expression regulation in zebra finch brain (Hilliard et al., 2012, their Table S2: only genes where *q*-values indicated significant support).

In addition, we mapped publicly available FOXP2-binding sequences on putative promoter sequences (5,000 bp upstream of transcription start) of the newly defined FOXP2 candidate genes. The down-loaded sequences were generated by chromatin immunoprecipitation with an antibody against 127 C-terminal aa of human FOXP2, followed by sequencing (FOXP2-ChIP-seq). The respective DNA was isolated from human neuroblastoma SK-N-MC cells (GEO project GSM803353: SRR351544; see also Nelson et al., 2013). The mapping results were normalized for the number of hits across the human genome (GRCh38.p7). The putative promoter sequences of the same genes were also screened for established FOXP2-binding motifs (see Stroud et al., 2006; Vernes et al., 2007, 2011; Nelson et al., 2013). This was done with the aid of SeqMap v. 1.0.3 (Jiang and Wong, 2008), without allowing for any mismatch.

Following others (e.g., Boeckx and Benítez-Burraco, 2014a,b) we employed the STRING server (v. 10.0⁵) for the reconstruction of a protein–protein interaction (PPI) network as well as for PPI enrichment and gene ontology (GO) enrichment analyses. Thresholds for the acceptance of a PPI were alternatively set to low (≥ 0.15), medium (≥ 0.4), high (≥ 0.7), and maximum combined confidence scores (≥ 0.9). We inferred node degree values per protein (= number of direct edges a protein has) with the aid of Cytoscape v. 3.2.1 and the plugin NetworkAnalyzer 1⁶.

We consulted brainspan.org for assessing spatiotemporal gene expression of new FOXP2 target genes in human brain. Sequences of all target genes (new and reproduced ones) and the encoded proteins can be retrieved from the ENSEMBL database via the identifiers (IDs) given in **Table 1**, amongst others. The same IDs lead to the rate ratios of synonymous to non-synonymous substitution rates (dN/dS) of the FOXP2 target genes and genes coding for interactors in the Rhesus monkey–human and Rhesus monkey–common chimpanzee comparison, which we retrieved from the ENSEMBL pages. The sampled dN/dS values were compared with a two-tailed Mann–Whitney *U* (MWU) test as implemented in

⁴<https://imagej.nih.gov/ij/index.html>

⁵<http://string-db.org>

⁶www.cytoscape.org

TABLE 1 | Proteins used for network reconstruction and GO enrichment analysis.

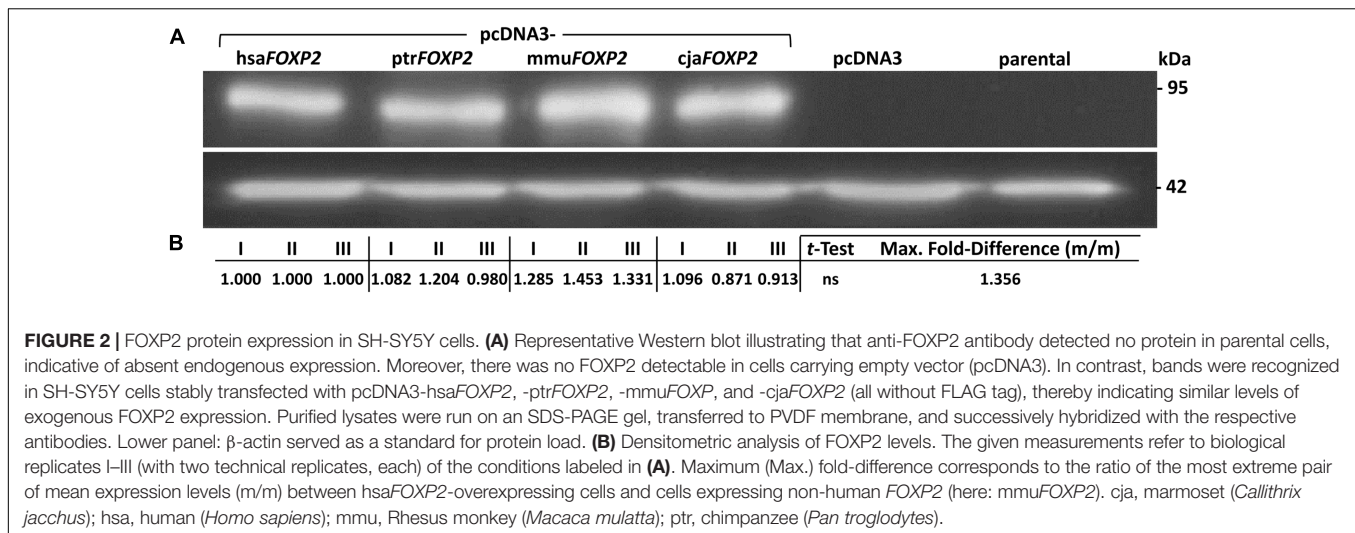
| Subsample | Symbol | ENSEMBL ID | Subsample | Symbol | ENSEMBL ID | |
|--|---------------------------------|-----------------|-------------------|-----------------|-----------------|-----------------|
| Encoded by reproduced FOXP2 targets | ADAP1 | ENSP00000265846 | Added interactors | CFTR | ENSP00000003084 | |
| | ALG11 | ENSP00000430236 | | DICER1 | ENSP00000343745 | |
| | APH1A | ENSP00000358105 | | EIF2C1 | ENSP00000362300 | |
| | CDH11 | ENSP00000268603 | | EIF2C2 | ENSP00000220592 | |
| | DNMBP | ENSP00000315659 | | EIF2C3 | ENSP00000362287 | |
| | ERP44 | ENSP00000262455 | | EIF2C4 | ENSP00000362306 | |
| | GPR160 | ENSP00000348161 | | EIF4E | ENSP00000425561 | |
| | HSD17B3 | ENSP00000364412 | | EIF4G1 | ENSP00000338020 | |
| | IFI30 | ENSP00000384886 | | EZR | ENSP00000338934 | |
| | IL4R | ENSP00000170630 | | HSP90AA1 | ENSP00000335153 | |
| | LONRF1 | ENSP00000381298 | | IL13 | ENSP00000304915 | |
| | LRP3 | ENSP00000253193 | | IL13RA1 | ENSP00000360730 | |
| | LRRTM2 | ENSP00000274711 | | IL2RG | ENSP00000363318 | |
| | MAFF | ENSP00000345393 | | IL4 | ENSP00000231449 | |
| | MARVELD1 | ENSP00000441365 | | JAK1 | ENSP00000343204 | |
| | MGST2 | ENSP00000265498 | | JAK2 | ENSP00000371067 | |
| | MRPS6 | ENSP00000382250 | | JAK3 | ENSP00000391676 | |
| | NEU1 | ENSP00000364782 | | KEAP1 | ENSP00000171111 | |
| | PCDHB16 | ENSP00000354293 | | KIF13B | ENSP00000427900 | |
| | PIM1 | ENSP00000362608 | | LRRK2 | ENSP00000298910 | |
| | SEMA6D | ENSP00000324857 | | MRPS10 | ENSP00000053468 | |
| | SERPINH1 | ENSP00000350894 | | MRPS16 | ENSP00000362036 | |
| | SETBP1 | ENSP00000282030 | | MRPS2 | ENSP00000241600 | |
| | TBX22 | ENSP00000362390 | | MRPS5 | ENSP00000272418 | |
| | TMEM5 | ENSP00000261234 | | NFATC1 | ENSP00000327850 | |
| | TNRC6C | ENSP00000336783 | | NFE2L2 | ENSP00000380252 | |
| | ZDHHC3 | ENSP00000296127 | | PABPC1 | ENSP00000313007 | |
| | Encoded by new FOXP2 targets | BACE2 | | ENSP00000332979 | PAIP1 | ENSP00000302768 |
| | | CDH4 | | ENSP00000353656 | PAN3 | ENSP00000370345 |
| | | DCDC2 | | ENSP00000367715 | RHOA | ENSP00000400175 |
| | | FOXL1 | | ENSP00000326272 | ROCK1 | ENSP00000382697 |
| | | GABRE | | ENSP00000359353 | SLC9A3R1 | ENSP00000262613 |
| | | MSN | | ENSP00000353408 | SOCS5 | ENSP00000305133 |
| MYH13 | | ENSP00000252172 | STAT3 | ENSP00000264657 | | |
| MYH8 | | ENSP00000384330 | STAT5A | ENSP00000341208 | | |
| NURR1 | | ENSP00000344479 | STAT5B | ENSP00000293328 | | |
| PHOX2B | | ENSP00000226382 | STAT6 | ENSP00000300134 | | |
| PTPRQ | | ENSP00000266688 | TARBP2 | ENSP00000266987 | | |
| SEBOX | | ENSP00000416240 | TNRC6A | ENSP00000379144 | | |
| TMEM200A | | ENSP00000296978 | TNRC6B | ENSP00000401946 | | |

SPSS (see above). *P*-values from *t*-tests (expressional analyses) were transformed into false discovery rates (FDRs), thus accounting for multiple testing (see, e.g., Vernes et al., 2007). FDRs in GO enrichment analysis as generated by Cytoscape were multiplied by the factor of two, thus conservatively adjusting for parallel testing of two datasets. *P*-values from PPI enrichment testing (network analysis) were adjusted in the same manner. Significance thresholds applied were <0.01 for GO enrichment analysis and <0.05 for all other tests. Data on sample sizes refer to the numbers of cell lines overexpressing either *hsaFOXP2* (N) or different non-human *FOXP2* cDNAs (M).

RESULTS

Evaluation of the Study System

RT-PCR detected only minimal endogenous *FOXP2* transcript in parental HEK293 cells (Supplementary Image 1). In further support of their suitability for subsequent validation steps, no *FOXP2* band appeared in lanes loaded with lysate from parental HEK293 cells (Western blotting). In contrast, anti-*FOXP2* antibody recognized protein bands of two different molecular weights in transiently transfected HEK293 cells, which overexpressed either human or one of the non-human primate *FOXP2* cDNAs. These differences correlated with



the extension and non-extension of the different FOXP2 sequences with a C-terminal FLAG tag, thus indicating full length transcription and translation of exogenously expressed FOXP2 (Supplementary Image 2). After having shown the functionality of the pcDNA3-FOXP2 constructs we turned to our actual study system, i.e., SH-SY5Y cells. RT-PCR confirmed previous notions of absent endogenous FOXP2 transcription in parental SH-SY5Y cells (Supplementary Image 1; see also, e.g., Zhao et al., 2015). Consistently, no FOXP2 protein was contained in lysates prepared from parental and pcDNA3-transfected SH-SY5Y cells, according to Western blotting (Figure 2). Thus, detection of FOXP2/FOXP2 in cells stably transfected with pcDNA3-FOXP2 constructs can be assigned to exogenous expression. Thereby, we ensured by Sanger sequencing that the different transfectants overexpressed the intended human, chimpanzee, Rhesus monkey, and marmoset FOXP2 cDNA, respectively (not shown). Notably, densitometric analysis suggested about equal FOXP2 protein amounts in hsaFOXP2-overexpressing cells on the one hand and SH-SY5Y cells transfected with ptrFOXP2, mmuFOXP2, and cjaFOXP2 cDNAs on the other (Figure 2). Consequently, downstream analyses of target gene expression levels should not be biased by unequal FOXP2 amounts across the cell lines compared.

Matching of RNA-seq Data with Results of Previous Studies

Preliminary analysis of BPKM values from present RNA-seq (GSE100291) revealed differential expression levels of altogether 898 genes in hsaFOXP2-overexpressing SH-SY5Y cells relative to the cells alternatively transfected with ptrFOXP2, mmuFOXP2, cjaFOXP2 cDNAs, and empty vector (biological replicates I and II per each condition). As to be expected from upstream experiments FOXP2 was not amongst these differentially regulated genes. However, the sample contained 122 genes that were previously reported to be potential FOXP2/Foxp2 targets (Spiteri et al., 2007; Vernes et al., 2007, 2011; Enard

et al., 2009; Konopka et al., 2009) and/or to have singing-related expression regulation in male zebra finch brain (Hilliard et al., 2012). In 27 out of these 122 reproduced genes support for differential BPKM levels under hsaFOXP2 control was significant according to FDRs <0.05 in the *t*-tests conducted (Supplementary Table 2.1). The corresponding *r* values indicated a large effect size (>0.5) for all 27 comparisons. Consequently, the test power estimates by G*Power constantly overshoot the threshold of acceptability, i.e., 80% (Supplementary Table 2.1). The detailed power estimates even ranged from 94 to 100% between the cells overexpressing hsaFOXP2 (*N* = 2) and non-human FOXP2 (*M* = 6). This fact, along with the appearance of these 27 genes in the reference studies, suggested that the inclusion of additional replicates should not alter the results. Consequently, we retained all 27 reproduced genes for downstream analyses (Supplementary Table 2.1 and Table 1).

New FOXP2 Targets and Validation by RT-qPCR

Subsequently, we addressed the question if the significance testing of RNA-seq data might have led to an underestimation of the extent of the (hsa)FOXP2-driven network. In order to get an estimate, we selected 13 additional genes out of the aforementioned preliminary set of 898 loci (Supplementary Table 2.2). The genes under scrutiny had low to moderate expression levels but at the same time showed more than twofold differential expression under hsaFOXP2 control relative to any other condition (mean *versus* mean). Furthermore, they were protein-coding and displayed expression in brain in at least some phase of human life⁷. The 13 genes selected did not receive significant statistical support for FOXP2/Foxp2-driven and/or songbird song-related expression regulation in any of the six reference studies mentioned in the previous paragraph. Thus, we herein refer to the respective genes as to new FOXP2 targets.

⁷brainspan.org

TABLE 2 | Target gene expression levels (RT-qPCR) in SH-SY5Y cells overexpressing human *FOXP2* relative to cells overexpressing non-human primate *FOXP2*.

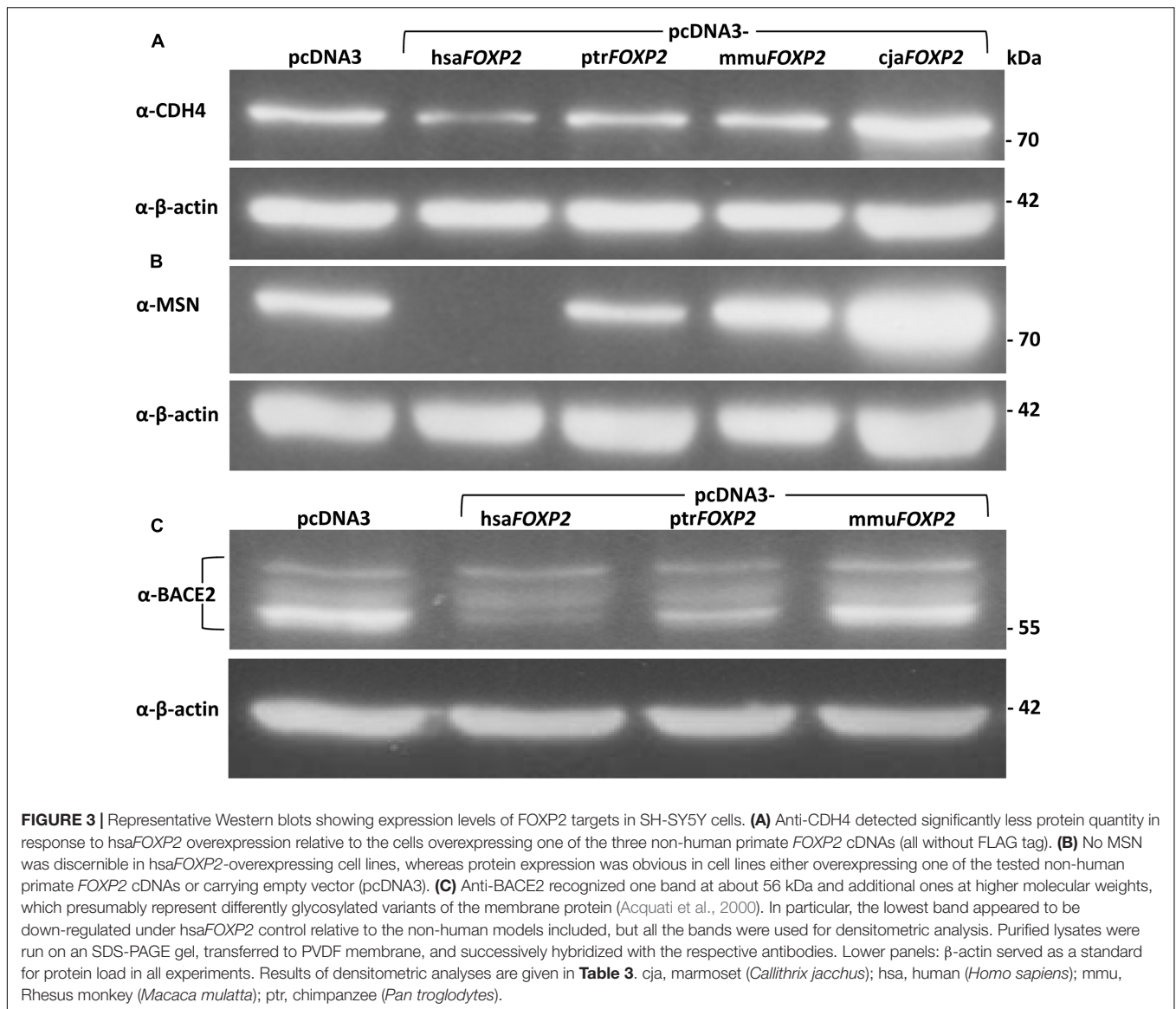
| Symbol | pcDNA3- | | | | | | | | FDR t-test | Min. fold- change (m/m) | <i>r</i> | Power |
|-----------------|----------|-------|----------|-------|---------|-------|----------|-------|---------------|----------------------------|----------|-------|
| | hsaFOXP2 | | ptrFOXP2 | | muFOXP2 | | cjaFOXP2 | | | | | |
| | I | II | I | II | I | II | I | II | | | | |
| <i>BACE2</i> | 0.177 | 0.211 | 1.875 | 1.973 | 1.598 | 1.999 | 0.595 | 0.497 | <0.001 | 0.355 | 0.735 | 0.725 |
| | 0.177 | 0.211 | 1.875 | 1.973 | 1.598 | 1.999 | – | – | <0.05 | 0.108 | 0.986 | 1.000 |
| <i>DCDC2</i> | 0.289 | 0.230 | 0.562 | 0.879 | 0.433 | 0.474 | 0.889 | 0.800 | <0.01 | 0.572 | 0.767 | 0.803 |
| <i>CDH4</i> | 0.284 | 0.387 | 1.128 | 1.661 | 3.003 | 3.565 | 2.437 | 2.154 | <0.05 | 0.241 | 0.808 | 0.895 |
| <i>FOXL1</i> | 0.378 | 0.308 | 3.404 | 2.443 | 3.140 | 3.661 | 2.235 | 1.790 | <0.001 | 0.170 | 0.897 | 0.997 |
| <i>GABRE</i> | 0.014 | 0.012 | 0.423 | 0.455 | 0.606 | 0.562 | 0.361 | 0.348 | <0.01 | 0.037 | 0.933 | 1.000 |
| <i>MSN</i> | 0.111 | 0.180 | 1.217 | 1.825 | 0.981 | 1.237 | 1.391 | 1.474 | <0.01 | 0.131 | 0.931 | 1.000 |
| <i>MYH8</i> | 0.253 | 0.293 | 1.369 | 1.620 | 1.337 | 1.285 | 1.974 | 2.067 | <0.01 | 0.208 | 0.923 | 1.000 |
| <i>MYH13</i> | 0.044 | 0.049 | 1.011 | 0.897 | 0.565 | 0.536 | 0.808 | 0.826 | <0.01 | 0.084 | 0.922 | 1.000 |
| <i>NURR1</i> | 0.092 | 0.131 | 2.742 | 2.331 | 3.386 | 3.915 | 0.840 | 1.007 | ns | 0.121 | 0.743 | 0.745 |
| | 0.092 | 0.131 | 2.742 | 2.331 | 3.386 | 3.915 | – | – | 0.01 | 0.044 | 0.943 | 0.999 |
| <i>PHOX2B</i> | 0.091 | 0.083 | 0.942 | 0.598 | 0.877 | 0.447 | 2.598 | 3.094 | <0.05 | 0.131 | 0.589 | 0.411 |
| | 0.091 | 0.083 | 0.942 | 0.598 | 0.877 | 0.447 | – | – | <0.05 | 0.131 | 0.873 | 0.899 |
| <i>PTPRQ</i> | 0.147 | 0.131 | 0.401 | 0.300 | 1.357 | 1.119 | 0.331 | 0.377 | <0.05 | 0.397 | 0.556 | 0.357 |
| | 0.147 | 0.131 | 0.401 | 0.300 | – | – | 0.331 | 0.377 | <0.01 | 0.397 | 0.950 | 1.000 |
| <i>SEBOX</i> | 4.423 | 4.172 | 0.105 | 0.143 | 0.143 | 0.169 | 0.153 | 0.182 | <0.05 | 25.657 | 0.998 | 1.000 |
| <i>TMEM200A</i> | 0.124 | 0.088 | 1.110 | 0.839 | 1.567 | 1.207 | 0.326 | 0.483 | ns | 0.262 | 0.731 | 0.715 |
| | 0.124 | 0.088 | 1.110 | 0.839 | 1.567 | 1.207 | – | – | <0.05 | 0.109 | 0.921 | 0.987 |

Two biological replicates (I, II) were measured per condition. Values were corrected for signal intensity of reference genes and normalized for expression levels in cells carrying empty expression vector. Minimum (Min.) fold-difference refers to the ratio of the least extreme pair of mean expression levels between hsaFOXP2-overexpressing cell lines and their counterparts overexpressing one of the non-human FOXP2 cDNA. Power estimates according to G*Power v. 3.1.9.2. FDR, false discovery rate; cja, marmoset (*Callithrix jacchus*); hsa, human (*Homo sapiens*); mmu, Rhesus monkey (*Macaca mulatta*); ns, not significant; ptr, chimpanzee (*Pan troglodytes*); *r*, correlation coefficient.

RT-qPCR confirmed up- (1 gene) and down-regulation (12 genes) of expression under hsaFOXP2 control in SH-SY5Y cells for all 13 genes measured (Table 2). The effect of hsaFOXP2 overexpression on target gene expression was again large, as indicated by *r*-values >0.5 in all of the comparisons between hsaFOXP2 and non-human FOXP2-overexpressing cells (biological replicates I and II per each condition). In twelve cases, RT-qPCR corroborated the results of RNA-seq of at least twofold up- or down-regulation (mean versus mean) under hsaFOXP2 control relative to any other condition. We noticed the strongest regulation in *SEBOX*, whereby the minimum fold-change between hsaFOXP2 and non-human primate FOXP2-overexpressing cells was >25 (with *N* = 2, *M* = 6), indicating a strong up-regulation of transcription in response to hsaFOXP2 overexpression (Table 2). The corresponding values for *BACE2*, *CDH4*, *FOXL1*, *GABRE*, *MSN*, *MYH8*, *MYH13*, *NURR1*, *PHOX2B*, *PTPRQ*, and *TMEM200A* ranged between 0.037 and 0.397, which corresponds to a considerable down-regulation of transcription for each of these loci. *DCDC2* failed the twofold-threshold in the comparison of the hsaFOXP2-overexpressing cells with any other condition (0.572) but down-regulation of expression under hsaFOXP2 control was nonetheless significant (Table 2). Significant FDRs (<0.05, *t*-test) were also reached in the human/non-human comparison of the other new FOXP2 target candidates, except for *NURR1* and *TMEM200A* (all with *N* = 2 and *M* = 6). The latter two genes missed the

5% threshold of significance in the first place, despite their strong down-regulation in hsaFOXP2-overexpressing cells and the correspondingly increased *r*-values (>0.7).

This discrepancy between effect size and significance testing in *NURR1* and *TMEM200A* apparently reflected an increased variation across the non-human models due to conspicuous values under cjaFOXP2 control. However, the inclusion of models for the Rhesus monkey and marmoset besides the chimpanzee condition was a rather conservative approach with respect to our prime goal of detecting expressional changes in the human model cell lines (compare Figure 1B). In *NURR1* and *TMEM200A*, the consideration of the complete species sample might even have obscured actually relevant changes in response to hsaFOXP2 overexpression. Accordingly, we found the expression levels of *NURR1* and *TMEM200A* to differ significantly under hsaFOXP2 control when the data were re-analyzed under exclusion of the values measured in the cjaFOXP2-overexpressing cells (thus, with *N* = 2 and *M* = 4; Table 2). The reduction in the species sample associated with an increase of the corresponding *r* values and power estimates for the *t*-tests carried out on *NURR1* and *TMEM200A*. Similarly, the power estimates overshoot the 80% threshold of acceptability when the levels of *BACE2*, *PHOX2B*, and *PTPRQ* transcripts were compared between hsaFOXP2-overexpressing cells and a reduced sample of non-human primate models (Table 2). Thus, *post hoc* analysis of *t*-tests underlined that significant support for expressional changes under hsaFOXP2



control could be correlated with acceptable power estimates in all 13 new target genes – at least after obscuring signal was excluded from the comparison. However, high power estimates suggest that the alternative hypothesis of unequal means (here: expression levels) is true. Consequently, additional biological replicates should reproduce the findings without bringing an essential gain of new information – a prediction that we tested on the protein level.

Western Blotting of Proteins Encoded by New FOXP2 Targets

The three proteins selected for Western blot analyses represented loci, for which the power of *t*-tests was >80% when contrasting transcript amounts (RT-qPCR) in *hsaFOXP2*-overexpressing SH-SY5Y cells with the corresponding levels in either the complete (*CDH4*, *MSN*) or a reduced set of non-human models (*BACE2*). Densitometric analysis confirmed significant down-regulation

under *hsaFOXP2* control for all three tested proteins, when taking the same two biological replicates per condition as used for transcriptome measurements (I and II). As in transcriptomic analyses, the *r* values exceeded the threshold of large effect size in all of the three comparisons of densitometric values (**Figure 3** and **Table 3**). Correspondingly, the power estimates for the conducted *t*-tests was constantly >80%, so that the inclusion of additional replicates should not alter the results. In line with this expectation, *t*-tests confirmed a significant down-regulation of protein expression after addition of a third biological replicate (III), thus increasing sample sizes to $N = 3$ and $M = 9$ for *CDH4* and *MSN*, and to $N = 3$ and $M = 6$ for *BACE2* (**Figure 3** and **Table 3**). We interpreted these findings as a confirmation that SH-SY5Y cells translated different transcript amounts of FOXP2 targets into corresponding protein quantities. The findings further demonstrated that large effect size and high power values appeared to be reliable predictors of the

TABLE 3 | Densitometric analyses of Western blots: CDH4, MSN, and BACE2 abundance in SH-SY5Y cells overexpressing human *FOXP2* relative to cells overexpressing non-human primate *FOXP2*.

| Protein | Overexpression of | | | | | | | | | | | | FDR <i>t</i> -test | <i>r</i> | Power |
|---------|-------------------|-------|-------|----------|-------|-------|----------|-------|-------|----------|-------|-------|--------------------|----------|-------|
| | hsaFOXP2 | | | ptrFOXP2 | | | mmuFOXP2 | | | cjaFOXP2 | | | | | |
| | I | II | III | I | II | III | I | II | III | I | II | III | | | |
| CDH4 | 0.431 | 0.650 | – | 0.952 | 1.171 | – | 1.018 | 1.045 | – | 1.336 | 1.213 | – | <0.01 | 0.861 | 0.976 |
| | 0.431 | 0.650 | 0.514 | 0.952 | 1.171 | 0.960 | 1.018 | 1.045 | 2.499 | 1.336 | 1.213 | 2.691 | <0.05 | – | – |
| MSN | 0.051 | 0.116 | – | 0.695 | 0.728 | – | 2.046 | 1.694 | – | 2.562 | 2.228 | – | <0.05 | 0.775 | 0.822 |
| | 0.051 | 0.116 | 0.077 | 0.695 | 0.728 | 0.595 | 2.046 | 1.694 | 1.759 | 2.562 | 2.228 | 2.204 | <0.001 | – | – |
| BACE2 | 0.358 | 0.348 | – | 0.749 | 0.731 | – | 1.071 | 0.989 | – | – | – | – | <0.001 | 0.900 | 0.958 |
| | 0.358 | 0.348 | 0.344 | 0.749 | 0.731 | 0.974 | 1.071 | 0.989 | 1.164 | – | – | – | <0.05 | – | – |

Two and three biological replicates per condition (I–III) were included in *t*-tests. Values were corrected for β -actin levels and normalized for protein levels of the respective protein in cells carrying empty vector. See **Figure 3** for representative Western blots. *cja*, marmoset (*Callithrix jacchus*); *hsa*, human (*Homo sapiens*); *mmu*, Rhesus monkey (*Macaca mulatta*); *ptr*, chimpanzee (*Pan troglodytes*).

reproducibility of *t*-test results, even when sample sizes were comparably small. In retrospect, therefore, the sample sizes in the transcriptome analyses seemed acceptable.

Mapping of FOXP2-Binding Motifs and FOXP2-ChIP-seq Reads to Putative Promoter Sequences of New FOXP2 Targets

After having shown differential expression under *hsaFOXP2* control for all 13 new candidate genes we investigated their regulatory sequences. Screening the 5 kb upstream the transcription start of the human orthologs we found numerous matches with publicly available FOXP2-ChIP-seq reads (SRR351544). The same putative promoter sequences additionally contained previously published FOXP2-binding motifs (see Stroud et al., 2006; Vernes et al., 2007; Nelson et al., 2013). The number of matches further increased when extra motifs overrepresented in murine *Foxp2* target gene promoters were taken into account (see Vernes et al., 2011). Overall, we detected between seven and 48 FOXP2/*Foxp2*-binding motifs within the putative human promoter sequences (Supplementary Table 2.3). Furthermore, we observed juxtaposition and overlaps of motifs and the matching positions of FOXP2-ChIP-seq reads in the promoter sequences of all 13 new target genes (see **Figure 4** for *CDH4*, *MSN*, and *BACE2*; see Supplementary Image 3 for the other genes). Thus, the expression of all 13 new candidate genes might be directly regulated by FOXP2. Whether in terms of a direct or indirect regulation through FOXP2 we accepted all 13 genes scrutinized for downstream network reconstruction.

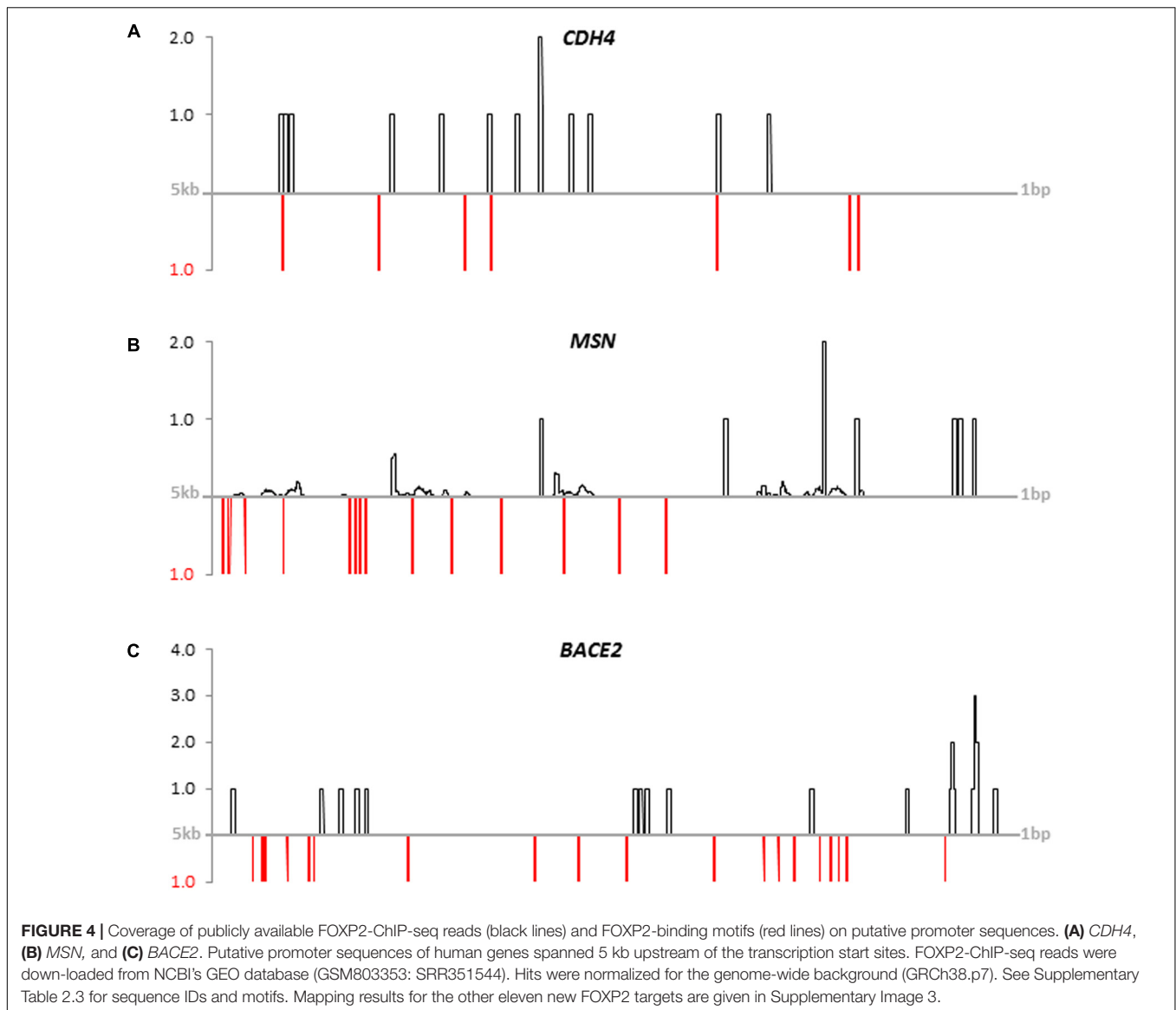
Network Reconstruction, Gene Ontology Enrichment Analysis, and Evolutionary Analysis

For network reconstruction, we merged our 13 new with the 27 reproduced target genes, thus generating an initial sample of 40 genes with empirical evidence for FOXP2/*Foxp2*-driven expression regulation. In order to reach a meaningful size for

network and GO analyses, the STRING server was enabled to add best-supported 40 interactors so that the final dataset contained 80 proteins (**Table 1** and Supplementary Tables 2.4, 2.5). Interestingly, these interactors contained nine additional proteins whose coding genes were previously shown to be FOXP2/*Foxp2* targets and/or to associate with singing in male zebra finch brains (Supplementary Table 2.4). Thus, altogether 49 nodes in the network correlated with empirical support for FOXP2/*Foxp2*-driven and/or songbird song-related expression regulation (nodes with rays in **Figure 5**). Disregarding six genes with only songbird song-related expression regulation a total of 43 nodes in our network associated with experimental evidence for FOXP2/*Foxp2*-driven expression regulation (**Table 1** and Supplementary Tables 2.1, 2.4). For this reason, we further refer to the network as to the FOXP2-driven network (**Figure 5**).

The number of PPIs was significantly increased relative to the expectation whichever confidence threshold was applied (*FDR* = 0, each; Supplementary Tables 2.6, 2.7). Fifty-three percent of the interactions were recognized with at least medium confidence (≥ 0.4). Confidence was still high (≥ 0.7) in 43% and highest (≥ 0.9) in 36% of the edges (**Figure 5** and Supplementary Table 2.7). Self-interactions were not detected. Six of the proteins were not engaged in any interaction. The remaining 74 proteins were constituents of the largest connected component (LCC), thereby having 11.342 PPI partners on average (see **Figure 5**). With 36 PPIs, the chaperone HSP90AA1 was the most connected protein in the LCC. Out of the new FOXP2 targets, MSN was the only one with an above-average node degree (= 15; **Figure 5** and Supplementary Table 2.6).

Kinases with high node degrees such as LRRK2 and Janus kinases JAK1-3 but also above-average connected PIM1 and average-connected ROCK1 pointed to a general involvement of our network in the regulation of protein activity. The same is true for ROCK1's highly connected upstream regulator RHOA, and for the phosphatase PTPRQ. Also the regulation of conductivity was represented by our network, namely through CFTR and GABRE (compare **Figure 5**; see Discussion for detailed protein functions). Additional functional implications emerged when testing our 80 protein sample for the enrichment



of GO terms (STRING). Applying a 1% FDR, 153 biological process GOs were overrepresented in our sample relative to the genome-wide background (Figure 5 and Supplementary Table 2.8). When individual terms were combined to larger entities, cellular signaling and communication appeared as the largest category (number of GO terms = 59; Figure 6 and Supplementary Table 2.8). This category contained members of the JAK/STAT cascade (statins, Janus kinases, and SOCS5) as well as MSN and EZR as constituents of the ezrin-radixin-moesin complex (ERM). Also cell-cell adhesion-mediating cadherins (*CDH4*, *CDH11*) were sorted into this category. Twenty-five GOs demonstrated importance for metabolic and catabolic processes as illustrated by *ZDDH3*, *KEAP1*, and *LRRK2*. Seventeen GOs reflected a strong involvement in transcriptional control (Figure 6). The latter category included transcriptionally active proteins like *MAFF*, *NFATC1*, and *TBX22* as well as proteins encoded by the new FOXP2 targets *NURR1*, *PHOX2B*, *FOXL1*,

and *SEBOX*. High relevance for post-transcriptional expression regulation was suggested by altogether eleven respective GOs. Proteins acting in ribosome recruitment (*EIF4E*, *EIF4G1*, and *PABPC1*) fell under this category. The same applied to highly connected *DICER1*, *TARBP2*, *TRNC6A-C*, and four RISC members (*EIF2C1-4*) which conjointly function in gene silencing. Actually, terms relating to gene silencing received the highest support from GO enrichment analysis (Supplementary Table 2.8). Five mitochondrial ribosomal proteins pointed to an engagement in protein synthesis as an additional layer of post-transcriptional expression regulation. Twenty-nine GOs indicated increased pertinence for development and cellular differentiation, migration, and motility. Notably, 10 out of these 29 GOs were directly relating to nervous system development and to neuron differentiation, projection, morphogenesis (inclusively axonogenesis and neurotrophin signaling) and survival (Figure 6). The 26 proteins matching

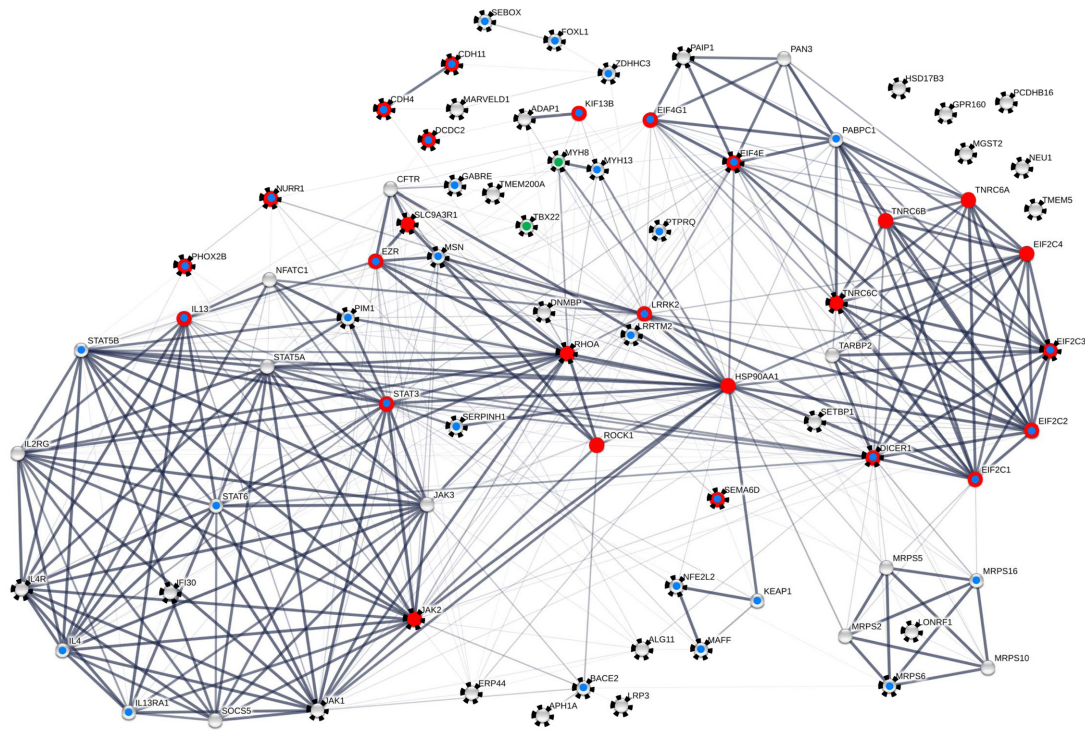


FIGURE 5 | FOXP2-driven protein–protein interaction (PPI) network including 80 proteins. Seventy-four nodes are contained in the largest connected component (LCC). Black rays highlight 49 proteins with empirical evidence for FOXP2/Foxp2-driven and/or songbird-song-related expression regulation from the present and previous analyses (see **Tables 2, 3** as well as Supplementary Tables 2.1, 2.4 for details). Red dots highlight proteins that matched with neuron-related GO terms in enrichment analysis (see Supplementary Table 2.8). Blue dots indicate nodes whose implication in neuronal and neural functions and/or diseases and disorders is detailed in the Discussion. This is a conservative estimate as exemplified by ERP44 which might have neural relevance (see Discussion) but is not categorized as such in this scheme. Green dots refer to an involvement in trismus-pseudocamptodactyly (MYH8) and X-linked cleft palate and ankyloglossia (TBX22). Proteins in the LCC have 11,342 direct interactors (node degree) on average. Thickness of edges correlates with confidence scores ≥ 0.90 , ≥ 0.7 , ≥ 0.4 , and ≥ 0.15 . The clustering coefficient varied between 0.616 and 0.831 depending on the confidence threshold applied. The network was constructed with the aid of STRING v. 10.0 and analyzed with the aid of Cytoscape v. 3.2.1 and the NetworkAnalyzer plugin. For individual node degrees and additional network statistics see Supplementary Tables 2.6, 2.7.

these “nervous system terms” are highlighted by red dots in **Figure 5** (compare Supplementary Table 2.8).

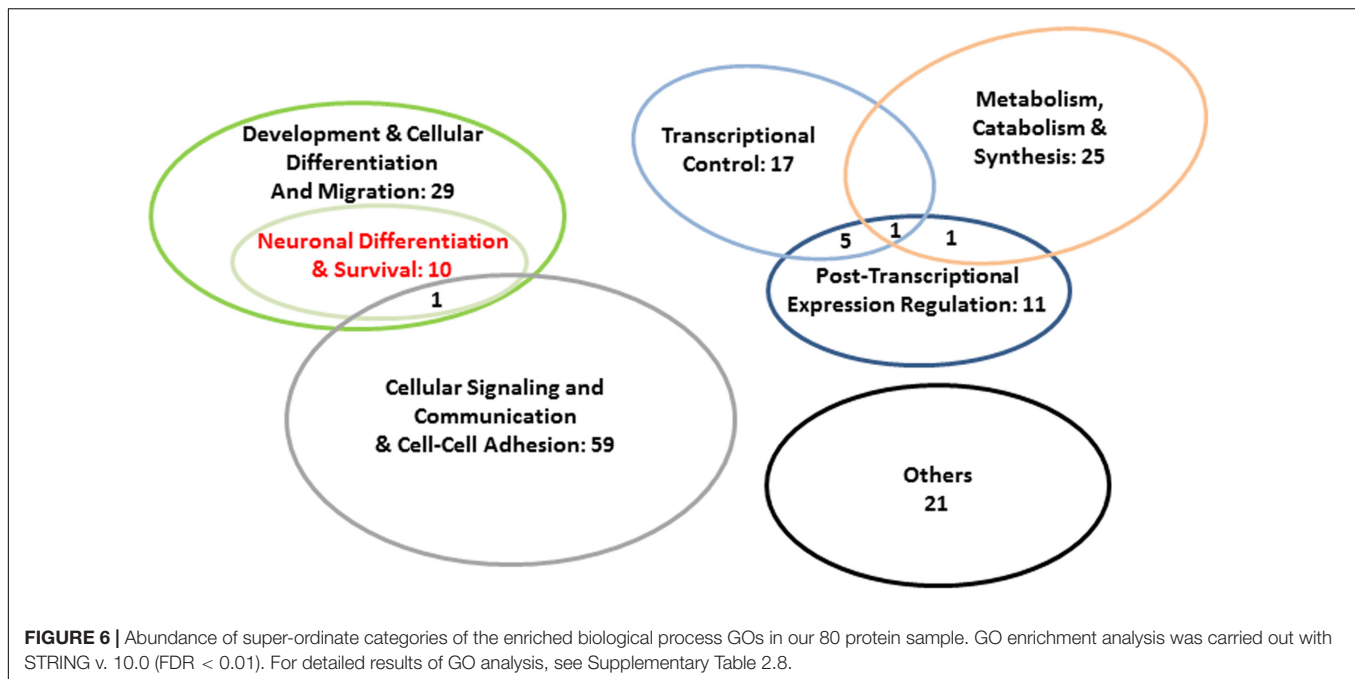
For assessing the impact of the newly detected FOXP2 targets we repeated network and GO enrichment analyses under exclusion of the respective 13 proteins, thus starting with the 27 reproduced loci only. After addition of 40 interactors STRING again detected significantly more nodes than expected, no matter which confidence threshold was applied (Supplementary Tables 3.1, 3.2). About 82% of the previously recognized enriched GO terms were also reproduced. However, with the exception of a single GO term (neurotrophin TRK receptor signaling pathway) there was no enrichment of terms literally relating to neuronal relevance anymore. In particular, terms containing the words “neuron” or “axonogenesis” were not enriched in the 67 protein sample (Supplementary Table 3.3). Thus, the inclusion of the new FOXP2 targets significantly affected the results of GO enrichment analysis.

Lastly, we analyzed the sequence evolution of the 80 protein sample on the basis of 59 protein-coding genes for which the respective values were available at the time of the study (ENSEMBL). Taking dN/dS as a measure we found overall similar

evolutionary rates in the Rhesus monkey–human and Rhesus monkey–chimpanzee comparison. This was evidenced at the level of mean dN/dS values (0.202 *versus* 0.200, respectively) as well as medians (0.148 *versus* 0.141, respectively; $P = 0.957$, MWU test). The single dN/dS values were all < 1.0 (Supplementary Table 2.9), thus illustrating that negative selection and hence selection against aa exchanges prevailed in the evolution of the present FOXP2-driven network.

DISCUSSION

Comparing human neuronal cells (SH-SY5Y) stably overexpressing species-specific primate *FOXP2* cDNAs, we detected 40 genes with differential expression levels in response to hsaFOXP2 overexpression. We refer to 27 of these genes as to reproduced FOXP2 targets as they have been already reported to show FOXP2/Foxp2-driven and/or songbird sing-related expression regulation in several reference studies (Spiteri et al., 2007; Vernes et al., 2007, 2011; Enard et al., 2009; Konopka et al., 2009; Hilliard et al., 2012). The remaining 13 genes with



differential expression levels controlled by *hsaFOXP2* did not show significantly differential regulation in any of the references and hence are termed new FOXP2 targets herein.

In support of the validity of the findings, *post hoc* analyses revealed that the recognition of transcriptional changes under *hsaFOXP2* control associated with acceptable power (>80%) of the conducted *t*-tests. This might be surprising on the first sight, considering that mRNA-based measurements involved comparably few cell lines modeling the human and non-human conditions, with a total sample size of mostly 8 and exceptionally 6 (Table 2 and Supplementary Table 2.1). However, such high power estimates fully agree with the results of a simulation study which demonstrated that *t*-tests can reach acceptable power despite small sample sizes ($N = 2; M = 5$; thus, with a total sample size of 7), when the corresponding effect sizes are high (de Winter, 2013). The precondition of large effect size was indeed fulfilled in present transcriptome analyses (Table 2 and Supplementary Table 2.1). As high power estimates suggest that the alternative hypothesis of unequal means is true, the inclusion of additional biological replicates should not have altered the results in present transcriptome analyses (see Cohen, 1988; Open Science Collaboration, 2012) – an assessment which we found confirmed for a selection of proteins encoded by new FOXP2 targets (Table 3). Therefore, it seemed justifiable to us to take all 40 genes which showed differential transcription under *hsaFOXP2* control as a starting sample for network reconstruction and evolutionary analysis.

The resulting FOXP2-driven network contained altogether 80 proteins. Matching the newly added interactors with the reference studies increased the number of nodes with FOXP2/*Foxp2*-driven and/or songbird song-related expression regulation in the network to a total of 49 (nodes with rays in Figure 5). Forty-three of them correlated with experimental evidence for

FOXP2/*Foxp2*-driven expression regulation from the present and several reference studies (see Results). Considering FOXP2's role in impairment of verbal communication (see Introduction), our FOXP2-driven network might have played a contributory role in human evolution, potentially even in the acquisition of speech and language (Figures 1, 5). However, adaptive aa substitutions were apparently of minor importance in this context as illustrated by prevalent signatures of negative selection, i.e., selection disfavoring aa exchanges, in genes coding for the proteins in our network (Supplementary Table 2.9). The codons of the respective genes might even evolve under stronger constraint than it is the case across the entire genome. Thus, the mean dN/dS of the genes encoding our network members was 0.202 in the Rhesus monkey-human comparison, while the genome-wide mean should be in the range of 0.26 or higher according to the dN and dS values, which Wolf et al. (2009) reported for the same species pair. This could point to an increased functional relevance of the FOXP2-driven network in primate evolution. If true, this seems to be a general principle as we observed similar evolutionary rates of the genes encoding our network members, whether the Rhesus monkey orthologs were compared with their counterparts in humans or common chimpanzee (Supplementary Table 2.9). On the contrary, our data do not suggest noteworthy changes in the evolutionary rates of the members of the FOXP2-driven network on the human branch (compare Figure 1B). This does not change the fact that adaptive evolution of some genes influenced hominization as it is the case for FOXP2 itself (Mallick et al., 2016; also, e.g., Enard et al., 2002; Mozzi et al., 2016). Still, present results of RNA-seq, RT-qPCR, and Western blotting rather emphasize the prominent role of expression regulation changes in human evolution (Tables 2, 3 and Supplementary Tables 2.1, 2.2), thus lending support to respective postulates from about 30 years ago

(e.g., King and Wilson, 1975). The changes in fine-tuning might have affected cellular signaling and communication, protein and nucleotide metabolism and catabolism, expression regulation, development and cellular differentiation and migration, and especially neuronal differentiation and survival (Figure 6). For reasons of space limitations we will focus in the following on the respective implications of the LCC in the present FOXP2-driven PPI network (Figure 5).

Cytoskeleton: MSN, the ERM Complex, and the Actin Scaffold

Above-average connected moesin (MSN, also MOE) was expressed at markedly lower levels in SH-SY5Y cells stably transfected with hsaFOXP2 relative to cells overexpressing non-human primate FOXP2 cDNAs (Figures 3B, 5 and Tables 2, 3). In support of its neuronal relevance, MSN protein levels were previously reported to be down-regulated in fetal Down syndrome brains (Lubec et al., 2001) whereas levels of a MSN-binding non-coding RNA (*MSNPIAS*) showed up-regulation in ASD cortices (Kerin et al., 2012). Such associations might reflect the central role of the protein in the remodeling of the cell cortex during mitosis and also its activation by the phosphatase PTEN (see Roubinet et al., 2011; also Georgescu et al., 2014). Hence, PTEN is a critical regulator of neuron development and survival, axonal regeneration, and synaptic plasticity and is implicated in AD, PD, and ALS (Ismail et al., 2012). Recent observations in the mouse model fit in with the presumed functional association of the three proteins. Thus, mislocalization of Pten in murine brain was observed to correlate with down-regulation of *Foxp2* and upregulation of *Msn* (Tilot et al., 2016).

Although MSN seems to function on its own (e.g., Fehon et al., 2010; Roubinet et al., 2011), it is also active through its participation in the ERM complex which additionally contains RDX and the present LCC member EZR (Figure 5). The ERM complex bridges the plasma membrane with the actin cytoskeleton, thus being involved in cell–cell recognition, signaling, and motility of diverse cell types as well as the formation and collapse of filopodia, microvilli, and microspikes (e.g., Fehon et al., 2010; Antoine-Bertrand et al., 2011; Roubinet et al., 2011; Georgescu et al., 2014). Accordingly, MSN and EZR matched in the present enrichment analysis with more general GO terms such as movement of cell or subcellular component and membrane to membrane docking (Supplementary Table 2.8). Nonetheless, the functional spectrum of the ERM complex also covers regulation of neurite outgrowth, neuron motility and growth cone morphology (e.g., Antoine-Bertrand et al., 2011 and references therein). These functions obviously substantiate the neuronal relevance of the present FOXP2-driven network – and of its LCC.

Activation of the complex through phosphorylation (pERM) involves three additional members of our LCC (Figure 5), i.e., RHOA, RHOA's downstream effector and regulator ROCK1 (Antoine-Bertrand et al., 2011; Tang et al., 2012), and LRRK2 (Parisiadou et al., 2009). ROCK1 is implicated in neuronal regeneration and neurite outgrowth (Da Silva et al., 2003; Tang et al., 2012). Moreover, mutations in *LRRK2* gene represent the most

frequent genetic cause of late-onset PD (Paisan-Ruiz et al., 2008), possibly due to negative effects on neurite outgrowth and survival of nigrostriatal dopaminergic neurons (Han et al., 2008; Xiao et al., 2015). The links between our LCC and neurodegeneration are even more manifest when considering that pERM is required for proteolytic processing of amyloid precursor protein (APP) by α -secretases into the neuroprotective soluble APP ectodomain (sAPP α) (Darmellah et al., 2012). Yet, the alternative cleavage of APP into neurotoxic amyloid- β (A β) is catalyzed by a γ -secretase containing present LCC member APH1A (Zhao et al., 2010) (Figure 5). Another APP processing pathway involves the aspartic protease encoded by the new FOXP2 target *BACE2* (β -site APP-cleaving enzyme 2; also *CEAP1*, *DRAP*) which resides inside the so-called 'Down critical region' in 21q22.3 (Acquati et al., 2000; O'Brien and Wong, 2011) (Figures 3C, 5 and Table 2). In line with the expectation for *BACE2*'s ability to cleave APP, certain variants of the coding gene associate with neurodegeneration, namely with AD (Myllykangas et al., 2005). However, the connections of our LCC with APP metabolism are not confined to the cleaving enzymes. Thus, the present LCC also contains the chaperone SERPINH1 (also HSP47) which has been demonstrated to regulate A β formation and the growth of amyloid plaques (Figure 5) (Bianchi et al., 2011).

Cytoskeleton: Myosins and Microtubules

The two myosin heavy chain proteins in the present LCC, both encoded by new FOXP2 targets (Figure 5 and Table 2), might have an influence on hard tissue development. Thus, *MYH8* levels were found to be up- and down-regulated in retrognathia and prognathia patients, respectively (Oukhai et al., 2011). Furthermore, a recurrent mutation in *MYH8* gene associates with trismus-pseudocamptodactyly syndrome (TPS) involving joint contracture and the inability of patients to open the mouth fully (also Dutch-Kentucky or Hecht-Beal syndrome; e.g., Toydemir et al., 2006). Strikingly, a recent study demonstrated the expression of *Foxp2* (and *Foxp1*) in the developing temporomandibular joint of mice (Cesario et al., 2016). Consequently, disturbed FOXP2-regulated expression of *MYH8* might indeed play a role in the pathogenesis of TPS. Also *MYH13* seems to be important for the development of the anatomical basis of speaking. The protein might especially be involved in the acquisition of adult larynx properties as suggested by cease of laryngeal *MYH13* expression during or after childhood (Périé et al., 2000). *MYH13* seems further to be involved in the pathogenesis of age-related neurodegenerative disorders (e.g., Cacabelos et al., 2012) and in formal thought disorder, or disorganized speech (Wang et al., 2012).

Besides, our FOXP2-driven network contributes to the organization of the microtubule scaffold. In particular, the new FOXP2 target *DCDC2* codes for a protein (Figure 5 and Table 2) which directs neuronal migration by stabilizing microtubules (e.g., Meng et al., 2005). This functional implication might have importance for human communication skills as suggested by mutations in *DCDC2* that associate with a recessive form of deafness (DFNB66), variation of gray matter volume in language-related brain regions of schizophrenia patients, reading disability (RD), and dyslexia (DYX2) (Meng et al., 2005; Jamadar

et al., 2011; Newbury et al., 2011; Grati et al., 2015). In line with these associations in humans, *DCDC2* is co-expressed in certain regions of the marmoset brain with other speech- and language-related genes like *FOXP2* itself, but also with *ROBO1*, *CMIP*, *KIAA03319*, and *CNTNAP2*. The spatiotemporal overlap includes thalamus and basal ganglia and, especially, substantia nigra pars compacta and pars reticulata (Kato et al., 2014; see also Vernes et al., 2008). Yet, nigrostriatal and thalamocortical-basal ganglia circuits function in voluntary motor control in marmoset (Kato et al., 2014) and dysfunction in humans can lead to oromandibular, lingual, and laryngeal spasms (Colosimo et al., 2010). Thus, *DCDC2* and the co-expressed speech- and language genes exemplify that the study of marmoset can improve our understanding of the molecular and neural basis of human communication. At the same time, *DCDC2* exemplifies that the differences in the communication skills between humans and marmoset might be due to changes in expression levels, which occurred on the human branch (compare **Figure 1B**).

Similar to *DCDC2*, *MARVELD1* has a rather peripheral position in our LCC. Nonetheless, also this protein has importance for the organization of microtubules as demonstrated for the murine ortholog (Zeng et al., 2011). Microtubules are further the basis for the functioning of present LCC member *KIF13B* (**Figure 5**). The protein moves along microtubules to the tips of neurites where it promotes neurite outgrowth (Yoshimura et al., 2010). Notably, the murine protein has been shown to be a negative regulator of PIK3K/AKT-mediated myelination in central and peripheral nervous system (Noseda et al., 2016). Yet, phosphatidylinositol-mediated signaling was one of the enriched GO terms in our protein sample (Supplementary Table 2.8). Moreover, PIK3K/AKT signaling could also link the new FOXP2 target *PTPRQ* (DFNB84A) (**Table 2**). The gene is another deafness susceptibility locus in our LCC (**Figure 5**) and codes for a phosphatidylinositol phosphatase (e.g., Schraders et al., 2010) which has been implicated in the organization of the actin cytoskeleton again (see, e.g., Nayak et al., 2007).

Transcriptional Regulation: Transcription Factors

A number of proteins in our LCC support FOXP2's previously stated influence on neuronal development and maintenance through downstream transcriptional regulators (**Figures 5, 6**). Thereby, the transcription factor encoded by the new FOXP2 target *NURR1* (also *NR4A2*, *NOT*) (**Figure 5** and **Table 2**) seems to be of special importance for normal dopaminergic functioning. Thus, stimulation of *NURR1* improves behavioral deficits associated with the degeneration of dopamine neurons in PD model mice – an effect which involves enhanced *trans*-repression of neurotoxic pro-inflammatory genes in microglia and increased transcriptional activation of midbrain dopaminergic (mDA) neurons (Kim et al., 2015). *Nurr1* knockout mice even fail to develop dopamine neurons (e.g., Zetterström et al., 1997). Therefore, it is not surprising that several mutations in human *NURR1* coincide with dopamine-related diseases, namely SCZD, Lewy body dementia (LBD), AD, and PD (e.g., Chen et al., 2001; Zheng et al., 2003; Chu et al., 2006). The involvement of the

present LCC in neuronal maintenance is also reflected by MAFF (**Figure 5**), i.e., another transcription factor, which has also been implicated in PD (reviewed in Kannan et al., 2012).

Four additional proteins further substantiate FOXP2's effectivity through downstream regulators of transcription (**Figures 5, 6** and see **Tables 2, 3** for new and reproduced FOXP2 targets). Corresponding evidence is particularly strong with respect to *PHOX2B*: Murine *Phox2b* regulates the differentiation of hindbrain visceral and branchial motor neurons (see Hirsch et al., 2013). *Phox2b* knockout mice even lack the facial motor nucleus which is an important source of Slit ligands for Robo receptor-expressing pontine neurons in wild-type mice (Geisen et al., 2008). Yet, the essentiality of SLIT1/ROBO signaling for neuron migration and axon guidance is well established (see, e.g., Geisen et al., 2008; Boeckx and Benítez-Burraco, 2014a,b; Pfenning et al., 2014), and *SLIT1* belongs to the already known FOXP2 targets (Konopka et al., 2009; Devanna et al., 2014). The second protein out of this group of four, *SEBOX* is involved in postnatal brain maturation as suggested by corresponding evidence in the mouse model (Cinquanta et al., 2000). Seeing the remarkable up-regulation of *SEBOX* under *hsaFOXP2* control (**Table 2**) the encoded protein might indeed have importance for human brain development and evolution. The third one, *FOXL1* could play a role in (mid)brain development as suggested by respective observations in the zebrafish (Nakada et al., 2006). Similarly, the functioning of the transcription factor *TBX22* has a morphogenetic dimension: Loss-of-function mutations in the coding gene cause X-linked cleft palate and ankyloglossia, a developmental disorder which decreases the motility of the tongue, thus leading to problems with feeding and speech. The disorder also affects dentition, hearing, and psychological development (Braybrook et al., 2001) Thus, the transcriptional cascades controlled by FOXP2 are essential for neural and neuronal maintenance and development as well as for normal development of the anatomical underpinning of speech.

Transcriptional Regulation: JAK/STAT Signaling

JAK/STAT signaling, represented in the present LCC by highly connected three Janus kinases (*JAK1-3*) and four statins (*STAT3*, *STAT5A*, *STAT5B*, *STAT6*) (**Figures 5, 6**), is commonly connoted with immune reaction (see Supplementary Table 2.8). However, a growing body of data points to a contributory role of the JAK/STAT cascade in the pathogenesis of Down syndrome, neuro-inflammatory diseases, and dopaminergic neurodegeneration (Lee et al., 2016; Qin et al., 2016). In agreement with the symptoms associated with these pathologies, present LCC members *STAT3*, *STAT5B*, and *STAT6* modulate neuron survival, synaptic plasticity, and neurite outgrowth (Deboy et al., 2006; Georganta et al., 2013; Tyzack et al., 2014).

The JAK/STAT cascade additionally includes interleukins, their receptors, and members of the suppressor of cytokine signaling (SOCS) protein family (also STAT-induced STAT inhibitor family). For example, interaction of *Socs5* with *Il4r* inhibits *Il4*-dependent activation of *Stat6* in the mouse model (Seki et al., 2002), and expression of *Il4* can again be induced by *Nfatc1* (Monticelli and Rao, 2002). Yet, the respective human

proteins belong to our LCC (**Figure 5**), thereby displaying about average to high connectivity.

Interestingly, the rodent orthologs of IL4 and of the second interleukin in our LCC, IL13, have been implicated in neuron survival, protection, and recovery (Pan et al., 2013; Walsh et al., 2015). IL4 and IL13 further share anti-inflammatory properties (Mori et al., 2016) and their common receptor comprises a subunit, IL13RA1 which has above-average connectivity in our network (**Figure 5**). The coding gene *IL13RA1* resides in the PD susceptibility locus PARK12 and its murine counterpart is expressed in dopaminergic neurons of the ventral tegmental area and the substantia nigra pars compacta (Morrison et al., 2012). Thus, also IL13RA1/*Il13ra1* relegate to dopaminergic neurodegeneration.

Confirmation of a JAK/STAT-mediated implication of our network and especially of the LCC in neuroprotection and neurodegeneration comes from HSP90AA1 (also HSP90). Not only that this chaperone had the most direct PIPs in our LCC but HSP90AA1 also interacts with STAT3 in human cells (Sato et al., 2003) (**Figure 5**). This again stabilizes the folding of another protein in our network, i.e., the phosphatase PIM1 (Shen et al., 2014), which once more builds the bridge to neuron survival: Pim1 inhibition rescues A β and Tau pathology in murine brain (Velazquez et al., 2016), and inhibition of human PIM1 induces the neuroprotective transcription factor NFE2L2 (also NRF2; McMahon et al., 2014). Yet, NFE2L2 and its inhibitor KEAP1 (see Yamazaki et al., 2015) are further components of the present LCC (**Figure 5**).

Post-transcriptional Expression Regulation

The present network and its LCC are additionally linked to gene silencing, namely through average- to highly connected proteins such as TARBP2, DICER1, and EIF2C1-4 (also AGO1-4) (**Figures 5, 6**; see also Vernes et al., 2011). This pathway will affect the expression of a wide range of indirect FOXP2 targets but also gene silencing of *FOXP2* itself is in the range of possible. In support of the latter, *Foxp2* showed premature expression in the embryonic neocortex of mice whose *Dicer* gene was knocked out (Clovis et al., 2012; but see Haesler et al., 2007). Whether in the one direction or just the other way around balanced gene silencing is certainly important for normal development. This is demonstrated by deletions involving *EIF2C1* and *EIF2C3* which were recently reported to associate with facial dysmorphologies, speech and motor delay, and also with moderate intellectual disability (Tokita et al., 2015). In addition, DICER1 and EIF2C2 appear to be connected with the pathogenesis of Huntington's disease (HD; e.g., Banez-Coronel et al., 2012; see also Batassa et al., 2010), thus providing an additional link between our LCC and dopamine imbalance (Chen et al., 2013).

The regulatory subunit PAN3 of the poly(A) nuclease PAN suggests an influence of our LCC on post-transcriptional expression regulation through mRNA decay (**Figures 5, 6**) (Uchida et al., 2004). The LCC is additionally pertinent to ribosome recruitment (compare, e.g., Vernes et al., 2011), as exemplified by PAIP1, PAIP1-binding PABPC1, and the highly connected eukaryotic translation initiation factors EIF4E and

EIF4G1 (e.g., Craig et al., 1998) (**Figure 5**). Yet, also ribosome recruitment is certainly vital for normal neural functioning as illustrated by late-onset motor incoordination in model mice upon sequestration of Pabpc1 (Damrath et al., 2012). Accordingly, mutations in *EIF4G1* have been recognized to associate with PD, and deregulation of *EIF4E* activity seems to increase susceptibility to autism (AUTS19) (Neves-Pereira et al., 2009; Chartier-Harlin et al., 2011).

Five moderately connected mitochondrial ribosomal subunits (MRPSs) underline that our LCC contributes to mitochondrial protein synthesis (**Figure 5**). The significance of this process for neuronal survival is exhibited by differential *MRPS6* levels in PD patients relative to unaffected individuals (Papapetropoulos et al., 2006). Moreover, a mutation in the *MRPS16* gene induces respiratory chain dysfunction with fatal consequences including agenesis of corpus callosum and death (Miller et al., 2004; Emdadul Haque et al., 2008). In further support of an effect of FOXP2 upon nervous system development through mitochondrial translation, murine isoform *Foxp2Ex12+* has been localized to mitochondria in Purkinje cells – especially in cellular buds giving rise to dendrites (Tanabe et al., 2012). Yet, Purkinje cells have been reported to show altered synapse plasticity in mice carrying humanized *Foxp2* (Reimers-Kipping et al., 2011).

Mitochondrial translation also builds the bridge to another LCC member, namely ERP44 (also Erp44; **Figure 5**). This chaperone regulates, along with other proteins, the association of mitochondria with the endoplasmic reticulum (ER). The establishment and maintenance of this interface is pivotal for cellular survival due to its influence on lipid transport, energy metabolism, and Ca²⁺ signaling (Hayashi et al., 2009). In particular, the latter implication might involve an inhibitory effect of ERP44 upon inositol-1,4,5-trisphosphate (IP3) receptors as demonstrated in mouse cerebellar microsomes (Higo et al., 2005). Yet, the implication of the LCC in phosphatidylinositol-mediated signaling was already mentioned, and Ca²⁺ release from the ER through IP3 receptors is altered in AD, HD, and ASD patients (see Schmunk et al., 2015 and references therein).

Membrane Conductivity and Cell–Cell Adhesion

Present evidence for differential regulation of *GABRE* under *hsaFOXP2* control corroborates previous findings stressing the importance of GABAergic circuitry for the evolution of speech and language (e.g., Boeckx and Benítez-Burraco, 2014a,b) (**Figure 5** and **Table 2**). *GABRE* shows wide tissue distribution but appropriately spliced mRNA was exclusively detected in the hypothalamic region and hippocampus and, to a much lesser degree, in heart tissue (Whiting et al., 1999). Consequently, *GABRE* might have more importance for nervous system functioning than known to date. Besides *GABRE*, it is ZDHHC3 (also GODZ) which links our LCC with GABAergic wiring (**Figure 5**). The Golgi-specific DHHC zinc finger protein palmitoylates the γ 2 subunit of GABA(A) receptors in neurons as demonstrated for the murine brain (Keller et al., 2004). Membrane conductivity is also modulated by present LCC member CFTR (**Figure 5**), which regulates chloride (and HCO₃-)

currents (Weyler et al., 1999). Interestingly, CFTR interacts with the abovementioned pERM and with another LCC member, i.e., SLC9A3R1 (also NHERF1) (Figure 5) (Alshafie et al., 2014). However, binding of SLC9A3R1 stabilizes the ERM complex and its kinase PTEN (Georgescu et al., 2014), whose neuronal and neural implications have been discussed above.

Importance for nervous system development through cell-cell adhesion has been found for diverse cadherins including CDH4 (also R-cadherin) which is encoded by one of the new FOXP2 targets (Figures 3A, 5 and Table 2; e.g., Oblander and Brady-Kalnay, 2010). Supporting the neural relevance of these Ca^{2+} -dependent proteins, CDH4 along with the gene coding for LCC member CDH11 (also OB-cadherin; Figure 5) was found to display differential spatial and temporal expression in developing marmoset brain (Matsunaga et al., 2015). In accordance, murine *Cdh4* and *Cdh11* seem to be essential for the association and migration of neurons during embryogenesis (Kimura et al., 1995; Hertel and Redies, 2011). Such relevance might partly reflect their interaction with other members of the cadherin family (e.g., Paulson et al., 2014). For instance, murine *Cdh4* interacts with *Cdh2* (N-cadherin) whose neuronal relevance is well-established (Matsunami et al., 1993). Moreover, *Cdh11* and *Cdh2* at least have overlapping functions including the regulation of β -catenin abundance and β -catenin-dependent gene expression (Di Benedetto et al., 2010). Yet, *Cdh2* is another *Foxp2* target, whose regulation has been shown to affect the detachment of differentiating neurons from the neuroepithelium (e.g., Rouso et al., 2012).

FOXP2's likely influence on neuronal development is further reflected by transmembrane LRRTM2, i.e., another member of the present LCC (Figure 5), which presumably regulates synapse formation through neurexin binding (Ko et al., 2009). An involvement in neurite formation and synapse formation is likewise probable for the transmembrane semaphorin SEMA6D (Figure 5) as suggested by observations in different model systems (e.g., Leslie et al., 2011). Congruously, the murine gene was previously reported to show *Foxp2*-driven expression regulation during neurite outgrowth (Vernes et al., 2011). It is thus unsurprising that SEMA6D matched with all neuron-related GO terms that were enriched in the present analysis, despite its peripheral position in our LCC (Figure 5 and Supplementary Table 2.8).

CONCLUSION

In the present study, we compared expression levels between SH-SY5Y cell lines stably overexpressing human FOXP2 cDNA with cell lines stably transfected with FOXP2 cDNAs of marmoset, macaque, and chimpanzee (Figure 1). Using RNA-seq, RT-qPCR, and Western blotting, we identified 13 new FOXP2 targets with differential expression levels under hsaFOXP2 control (Tables 2, 3; also Figure 3). The putative promoter sequences of all new target genes contained previously published FOXP2/FOXP2-binding motifs. Multiple matches of publicly available FOXP2-ChIP-seq reads with fragments inside the same promoter sequences additionally pointed to a potential direct binding of

FOXP2. Thus, down-regulation of expression might reflect that hsaFOXP2 represses the respective target genes more efficiently than any of the non-human FOXP2s studied. The opposite might be true for transcription of *SEBOX*, the only gene amongst the new targets that showed hsaFOXP2-driven up-regulation. Whether their transcription is directly or indirectly regulated by FOXP2, the detection of 13 new targets denotes that the extent of the FOXP2-driven network is greater than currently known. It is further conceivable that the extent of the FOXP2-driven network was underestimated so far especially at the expense of target genes with moderate or even low transcription rates.

The 13 new FOXP2 targets, along with 27 reproduced ones set the start point for the reconstruction of a PPI network (Figure 5). The resulting network contained in total 80 proteins, thereof 43 with confirmed experimental evidence for FOXP2/*Foxp2*-driven expression regulation. Altogether 49 proteins in the network showed FOXP2/*Foxp2*-driven and/or songbird song-related expression regulation (Figure 3, Tables 2, 3, and Supplementary Tables 2.1, 2.4; see also Spiteri et al., 2007; Vernes et al., 2007, 2011; Hilliard et al., 2012). In-depth literature screening and GO analysis underlined a general pattern showing that FOXP2 is effective also indirectly through signaling cascades and other transcriptionally and post-transcriptionally active proteins (Figure 6 and Supplementary Table 2.8; also, e.g., Marcus and Fisher, 2003; Konopka et al., 2009). Additional functional domains whose fine-tuning might have had a considerable effect on hominization are as follows: regulation of cellular signaling and communication, protein and nucleotide metabolism and catabolism, as well as cellular migration, differentiation and development inclusively neuronal differentiation and survival (Figure 6). In particular, the neural and neuronal relevance of FOXP2 was demonstrated before (see, e.g., Enard et al., 2009; Konopka et al., 2009). However, the present study illustrates that also less connected proteins with only moderate to low expression levels can significantly alter our understanding of FOXP2's role in neural and neuronal development, maintenance, and functioning: Thus, GO terms including the words "neuron" or "axonogenesis" (thus excluding "neurotrophin") only appeared to be enriched as long as the 13 new FOXP2 targets were included (compare Supplementary Tables 2.8, 3.3). Nonetheless, the numerous connections between the present network and neuritogenesis, neuron differentiation, etc. were by no means restricted to the new FOXP2 targets (see Discussion for details).

It is further worthwhile that we identified comparably few genes (see present Supplementary Table 2.1: genes without significant support) that were previously reported as differentially expressed between SH-SY5Y cells overexpressing either human FOXP2 cDNA or a "chimpanized" variant (*FOXP2*^{chimp}; see Konopka et al., 2009, their Supplementary Table 1). The same applies with respect to an earlier examination of the effect of the two human-specific aa substitutions in mice carrying humanized *Foxp2* (*Foxp2*^{hum}; see Enard et al., 2009; their Figures S8A,B, right panel). On the contrary, the overlap was much higher between the present protein sample and the lists of targets that were identified by FOXP2-ChIP-seq in human tissues and in SH-SY5Y cells stably overexpressing human FOXP2 (Spiteri et al., 2007, their Table 1; Vernes et al., 2007; their Table 1). The

overlap increased when expanding the comparison to *Foxp2* targets identified by ChIP-seq in wild type murine brain (Vernes et al., 2011, their Table S1). The number of reproduced loci further rose when genes with songbird song-related expression regulation were considered (Hilliard et al., 2012, their Table S2). These differences in overlap might partially reflect the different size of the gene lists taken as references. Nonetheless, there seems to be a trend displaying that we primarily re-identified genes from the studies that used non-mutated cDNAs rather than mutated ones combining states of two species. From our point of view this supports the suitability of species-specific cDNAs with counterparts in nature for studying FOXP2's role in evolution.

The present study differs from others especially with respect to the phylogenetic concept applied. Yet, this conceptual extension is not only of theoretical value as illustrated by the special case of *PHOX2B*. This gene was already a candidate for FOXP2-mediated expression regulation in a previous study which compared expression levels in SH-SY5Y cells overexpressing human FOXP2 versus cells carrying empty vector (Spiteri et al., 2007). Although RT-qPCR indicated down-regulation of transcription in the overexpressing cells the difference was not significant. In contrast, the present approach yielded significant support for down-regulation of *PHOX2B* expression in hsaFOXP2-overexpressing cells relative to cells overexpressing ptrFOXP2 and mmuFOXP2. In our opinion this illustrates the usefulness of a phylogenetic approach including at least one additional non-human model besides human and chimpanzee models in order to unmask changes in the fine-tuning of target gene expression that might have importance for human evolution and health.

In this way, we determined multiple connections of the FOXP2-driven network and its LCC to developmental (ASD, SCZD, Down syndrome, agenesis of corpus callosum, trismus-pseudocamptodactyly, ankyloglossia, facial dysmorphology) and neurodegenerative disorders and diseases (AD, PD, HD, LBD, ALS), deafness, and dyslexia (for details, see Discussion). In particular, the links to AD, PD, and HD pathologies but also diverse connections to the affected neuron types and brain regions substantiate the importance of FOXP2 for dopaminergic wiring and neurodegeneration (see Discussion for details; also, e.g., Reimers-Kipping et al., 2011; Hilliard et al., 2012; Devanna et al., 2014; Pfenning et al., 2014; Schreiweis et al., 2014). Moreover, reported communication deficits in at least some cases of AD, PD, HD, LBD, ALS, ASD, SCZD, and Down syndrome (Murray, 2000; Yoder and Warren, 2004; Stephane et al., 2007; Abrahams and Geschwind, 2010; Kupferberg, 2010; Reilly et al., 2010; Ferris and Farlow, 2013) confirm the well-established involvement of FOXP2 in the evolutionary and developmental acquisition of speech and language (see, e.g., Vernes and Fisher, 2009; Bolhuis et al., 2010; Enard, 2011; but see Mallick et al., 2016).

However, the present approach did not only confirm and substantiate previous knowledge. Thus, we were able to delineate new pathways of how human FOXP2 governs neurogenesis, neurite outgrowth, synapse plasticity, neuron migration, and the regulation of conductivity. These involve:

(i) transcription regulation through NURR1, PHOX2B, TBX22, SEBOX, and FOXL1, (ii) cadherin-mediated cell-cell adhesion (CDH4, CDH11), (iii) gene silencing through DICER1 and RISC, (iv) JAK/STAT signaling and neuro-inflammation, and (v) the organization of the microtubule (DCDC2, KIF13B), myosin (MYH8, MYH13), and actin cytoskeleton (PTPRQ, MSN and ERM complex). Single interactors of gene silencing, the ERM complex and JAK/STAT signaling also appeared in other FOXP2-directed studies (e.g., RDX in Figure 3 of Konopka et al., 2009; Dicer1 and Jak1 in Table S1 of Vernes et al., 2011). Yet, such implications of FOXP2 seemingly did not emerge with the same clarity before. In this way, we regard also gene silencing, JAK/STAT signaling, and the regulation of the ERM complex as novel FOXP2-driven pathways.

We hope that these novel insights may open up new avenues toward a better understanding of the molecular causes of the aforementioned developmental disorders, of communication deficits and especially of neurodegenerative diseases. With respect to the latter it would be advantageous to further investigate if down-regulation of newly detected FOXP2 targets such as *DCDC2*, *MYH8*, and *MYH13* under hsaFOXP2 control is due to direct FOXP2-binding. FOXP2-ChIP-qPCR could be a good way to answer this question, and also for validating the expressional differences which we observed in RNA-seq, RT-qPCR, and Western blot analyses. The entire spectrum of techniques could further be applied to transiently transfected SH-SY5Y cells, which overexpress different primate FOXP2 cDNAs. Reproduction of our findings in such cell lines would rule out that inestimable effects of the foreign DNA integrates (pcDNA3-constructs) into the genomes of SH-SY5Y cells have biased our results. This seems especially relevant considering that the integration sites and the number of integrated plasmids can vary between stably transfected cells and their descendants, due to the random integration of plasmids (e.g., Mitin et al., 2001). In genes such as *PHOX2B* and *NURR1* further steps could involve animal studies to verify if their established implication in brain development and maintenance is FOXP2-driven or not. Lastly, in cases where the present study evidenced down-regulated expression at the protein level (CDH4, MSN, BACE2) the next steps could involve the investigation of murine knock-outs against the background of neurodegenerative disease phenotypes. Preliminary data on *Cdh4* seem promising in this respect: A viable knock-out reportedly decreased activity, amongst others (see MGI:99218). However, if this change ultimately reflects changes in *Foxp2* expression or *Foxp2* activity and if the behavioral data associate with an alteration in neuronal wiring are questions waiting for an answer.

AUTHOR CONTRIBUTIONS

FO, PK, and AR generated the pcDNA3-FOXP2 constructs and cultivated, transfected, and characterized HEK293 and SH-SY5Y cells. The same authors carried out immunoblotting and densitometric analysis. BH, UZ, and HH conducted and analyzed RT-qPCR measurements. DR and HH analyzed

RNA-seq data as well as previously published FOXP2-ChIP-seq data, and searched putative target gene promoters for established FOXP2/FOXP2-binding motifs. FB assisted in data analysis. HH conducted network reconstruction, gene ontology analysis, in-depth literature screening, and evolutionary analysis. HH, UZ, FO, and SR conceived the study. HH wrote the manuscript. SR, FO, UZ, DR, and FB co-wrote the manuscript. All authors were involved in the scientific interpretation of the results.

FUNDING

This work was supported by the German Research Foundation (DFG, collaborative research grant SFB 1074/A3), and by the BMBF (research nucleus SyStAR) to FO.

REFERENCES

- Abrahams, B. S., and Geschwind, D. H. (2010). Connecting genes to brain in the autism spectrum disorders. *Arch. Neurol.* 67, 395–399. doi: 10.1001/archneurol.2010.47
- Acquati, F., Accarino, M., Nucci, C., Fumagalli, P., Jovine, L., Ottolenghi, S., et al. (2000). The gene encoding DRAP (BACE2), a glycosylated transmembrane protein of the aspartic protease family, maps to the down critical region. *FEBS Lett.* 468, 59–64. doi: 10.1016/S0014-5793(00)01192-3
- Adegbola, A. A., Cox, G. F., Bradshaw, E. M., Hafler, D. A., Gimelbrant, A., and Chess, A. (2015). Monoallelic expression of the human *FOXP2* speech gene. *Proc. Natl. Acad. Sci. U.S.A.* 112, 6848–6854. doi: 10.1073/pnas.1411270111
- Alshafie, W., Chappe, F. G., Li, M., Anini, Y., and Chappe, V. M. (2014). VIP regulates CFTR membrane expression and function in Calu-3 cells by increasing its interaction with NHERF1 and P-ERM in a VPAC1- and PKCepsilon-dependent manner. *Am. J. Physiol. Cell. Physiol.* 307, C107–C119. doi: 10.1152/ajpcell.00296.2013
- Antoine-Bertrand, J., Ghogha, A., Luangrath, V., Bedford, F. K., and Lamarche-Vane, N. (2011). The activation of ezrin-radixin-moesin proteins is regulated by netrin-1 through Src kinase and RhoA/Rho kinase activities and mediates netrin-1-induced axon outgrowth. *Mol. Biol. Cell* 22, 3734–3746. doi: 10.1091/mbc.E10-11-0917
- Banez-Coronel, M., Porta, S., Kagerbauer, B., Mateu-Huertas, E., Pantano, L., Ferrer, I., et al. (2012). A pathogenic mechanism in Huntington's disease involves small CAG-repeated RNAs with neurotoxic activity. *PLoS Genet.* 8:e1002481. doi: 10.1371/journal.pgen.1002481
- Batassa, E. M., Costanzi, M., Saraulli, D., Scardigli, R., Barbato, C., Cogoni, C., et al. (2010). RISC activity in hippocampus is essential for contextual memory. *Neurosci. Lett.* 471, 185–188. doi: 10.1016/j.neulet.2010.01.038
- Bianchi, F. T., Camera, P., Ala, U., Imperiale, D., Migheli, A., Boda, E., et al. (2011). The collagen chaperone HSP47 is a new interactor of APP that affects the levels of extracellular beta-amyloid peptides. *PLoS ONE* 6:e22370. doi: 10.1371/journal.pone.0022370
- Boeckx, C., and Benítez-Burraco, A. (2014a). Globularity and language-readiness: generating new predictions by expanding the set of genes of interest. *Front. Psychol.* 5:1324. doi: 10.3389/fpsyg.2014.01324
- Boeckx, C., and Benítez-Burraco, A. (2014b). The shape of the language-ready brain. *Front. Psychol.* 5:282. doi: 10.3389/fpsyg.2014.00282
- Bolhuis, J. J., Okanoya, K., and Scharff, C. (2010). Twitter evolution: converging mechanisms in birdsong and human speech. *Nat. Rev. Neurosci.* 11, 747–759. doi: 10.1038/nrn2931
- Bowers, J. M., and Konopka, G. (2012). The role of the FOXP family of transcription factors in ASD. *Dis. Markers* 33, 251–260. doi: 10.3233/DMA-2012-0919
- Braybrook, C., Doudney, K., Marciano, A. C., Arnason, A., Bjornsson, A., Patton, M. A., et al. (2001). The T-box transcription factor gene *TBX22* is mutated in X-linked cleft palate and ankyloglossia. *Nat. Genet.* 29, 179–183. doi: 10.1038/ng730
- Bruce, H. A., and Margolis, R. L. (2002). *FOXP2*: novel exons, splice variants, and CAG repeat length stability. *Hum. Genet.* 111, 136–144. doi: 10.1007/s00439-002-0768-5
- Cacabelos, R., Martinez, R., Fernandez-Novoa, L., Carril, J. C., Lombardi, V., Carrera, I., et al. (2012). Genomics of dementia: *APOE*- and *CYP2D6*-related pharmacogenetics. *Int. J. Alzheimers Dis.* 2012:518901. doi: 10.1155/2012/518901
- Cesario, J. M., Almaidhan, A. A., and Jeong, J. (2016). Expression of forkhead box transcription factor genes *Foxp1* and *Foxp2* during jaw development. *Gene Expr. Patterns* 20, 111–119. doi: 10.1016/j.gep.2016.03.001
- Chartier-Harlin, M.-C., Dachsel, J. C., Vilarino-Guell, C., Lincoln, S. J., LePrete, F., Hulihan, M. M., et al. (2011). Translation initiator *EIF4G1* mutations in familial Parkinson disease. *Am. J. Hum. Genet.* 89, 398–406. doi: 10.1016/j.ajhg.2011.08.009
- Chen, J. Y., Wang, E. A., Capeda, C., and Levine, M. S. (2013). Dopamine imbalance in Huntington's disease: a mechanism for the lack of behavioral flexibility. *Front. Neurosci.* 7:114. doi: 10.3389/fnins.2013.00114
- Chen, Y. H., Tsai, M. T., Shaw, C. K., and Chen, C. H. (2001). Mutation analysis of the human *NR4A2* gene, an essential gene for midbrain dopaminergic neurogenesis, in schizophrenic patients. *Am. J. Med. Genet.* 105, 753–757. doi: 10.1002/ajmg.10036
- Chu, Y., Le, W., Kompolti, K., Jankovic, J., Mufson, E. J., and Kordower, J. H. (2006). *Nurr1* in Parkinson's disease and related disorders. *J. Comp. Neurol.* 494, 495–514. doi: 10.1002/cne.20828
- Cinquanta, M., Rovescalli, A. C., Kozak, C. A., and Nirenberg, M. (2000). Mouse *Sebox* homeobox gene expression in skin, brain, oocytes, and two-cell embryos. *Proc. Natl. Acad. Sci. U.S.A.* 97, 8904–8909. doi: 10.1073/pnas.97.16.8904
- Clovis, Y. M., Enard, W., Marinaro, F., Huttner, W. B., and De Pietri Tonelli, D. (2012). Convergent repression of *Foxp2* 3'UTR by miR-9 and miR-132 in embryonic mouse neocortex: implications for radial migration of neurons. *Development* 139, 3332–3342. doi: 10.1242/dev.078063
- Cohen, J. (1988). *Statistical Power Analysis for the Behavioral Sciences*, 2nd Edn. New York, NY: Lawrence Erlbaum Associates.
- Colosimo, C., Suppa, A., Fabbrini, G., Bologna, M., and Berardelli, A. (2010). Craniocervical dystonia: clinical and pathophysiological features. *Eur. J. Neurol.* 17(Suppl. 1), 15–21. doi: 10.1111/j.1468-1331.2010.03045.x
- Craig, A. W., Haghighat, A., Yu, A. T., and Sonenberg, N. (1998). Interaction of polyadenylate-binding protein with the eIF4G homologue PAIP enhances translation. *Nature* 392, 520–523. doi: 10.1038/33198
- Da Silva, J. S., Medina, M., Zuliani, C., Di Nardo, A., Witke, W., and Dotti, C. G. (2003). RhoA/ROCK regulation of neuriteogenesis via profilin II-mediated control of actin stability. *J. Cell. Biol.* 162, 1267–1279. doi: 10.1083/jcb.200304021

ACKNOWLEDGMENTS

We want to thank S. Schirmer and R. Rittelmann (University Medical Center Ulm, Germany) for excellent technical assistance. Our thanks go further to H. Zischler (Institut für Organismische und Molekulare Evolutionsbiologie, Mainz, Germany) for fruitful discussions. We apologize to all whose contributions could not be cited for reasons of space limitations.

SUPPLEMENTARY MATERIAL

The Supplementary Material for this article can be found online at: <http://journal.frontiersin.org/article/10.3389/fncel.2017.00212/full#supplementary-material>

- Damrath, E., Heck, M. V., Gispert, S., Azizov, M., Nowock, J., Seifried, C., et al. (2012). ATXN2-CAG42 sequesters PABPC1 into insolubility and induces FBXW8 in cerebellum of old ataxic knock-in mice. *PLoS Genet.* 8:e1002920. doi: 10.1371/journal.pgen.1002920
- Darmellah, A., Rayah, A., Auger, R., Cuif, M.-H., Prigent, M., Arpin, M., et al. (2012). Ezrin/radixin/moesin are required for the purinergic P2X7 receptor (P2X7R)-dependent processing of the amyloid precursor protein. *J. Biol. Chem.* 287, 34583–34595. doi: 10.1074/jbc.M112.400010
- de Winter, J. C. F. (2013). Using the Student's t-test with extremely small sample sizes. *Pract. Assess. Res. Eval.* 18, 1–12.
- Debatisse, M., Toledo, F., and Anglana, M. (2004). Replication initiation in mammalian cells: changing preferences. *Cell Cycle* 3, 19–21. doi: 10.4161/cc.3.1.628
- Deboy, C. A., Xin, J., Byram, S. C., Serpe, C. J., Sanders, V. M., and Jones, K. J. (2006). Immune-mediated neuroprotection of axotomized mouse facial motoneurons is dependent on the *IL-4/STAT6* signaling pathway in CD4(+) T cells. *Exp. Neurol.* 201, 212–224. doi: 10.1016/j.expneurol.2006.04.028
- Devanna, P., Middelbeek, J., and Vernes, S. C. (2014). FOXP2 drives neuronal differentiation by interacting with retinoic acid signaling pathways. *Front. Cell. Neurosci.* 8:305. doi: 10.3389/fncel.2014.00305
- Di Benedetto, A., Watkins, M., Grimston, S., Salazar, V., Donsante, C., Mbalaviele, G., et al. (2010). N-cadherin and cadherin 11 modulate postnatal bone growth and osteoblast differentiation by distinct mechanisms. *J. Cell Sci.* 123, 2640–2648. doi: 10.1242/jcs.067777
- Emdadul Haque, M., Grasso, D., Miller, C., Spremulli, L. L., and Saada, A. (2008). The effect of mutated mitochondrial ribosomal proteins S16 and S22 on the assembly of the small and large ribosomal subunits in human mitochondria. *Mitochondrion* 8, 254–261. doi: 10.1016/j.mito.2008.04.004
- Enard, W. (2011). FOXP2 and the role of cortico-basal ganglia circuits in speech and language evolution. *Curr. Opin. Neurobiol.* 21, 415–424. doi: 10.1016/j.conb.2011.04.008
- Enard, W., Gehre, S., Hammerschmidt, K., Holter, S. M., Blass, T., Somel, M., et al. (2009). A humanized version of Foxp2 affects cortico-basal ganglia circuits in mice. *Cell* 137, 961–971. doi: 10.1016/j.cell.2009.03.041
- Enard, W., Przeworski, M., Fisher, S. E., Lai, C. S. L., Wiebe, V., Kitano, T., et al. (2002). Molecular evolution of FOXP2, a gene involved in speech and language. *Nature* 418, 869–872. doi: 10.1038/nature01025
- Fan, H.-C., Ho, L.-I., Chi, C.-S., Chen, S.-J., Peng, G.-S., Chan, T.-M., et al. (2014). Polyglutamine (PolyQ) diseases: genetics to treatments. *Cell Transplant.* 23, 441–458. doi: 10.3727/096368914X678454
- Faul, F., Erdfelder, E., Buchner, A., and Lang, A. G. (2009). Statistical power analyses using G*Power 3.1: tests for correlation and regression analyses. *Behav. Res. Methods* 41, 1149–1160. doi: 10.3758/BRM
- Fehon, R. G., McClatchey, A. I., and Bretscher, A. (2010). Organizing the cell cortex: the role of ERM proteins. *Nat. Rev. Mol. Cell Biol.* 11, 276–287. doi: 10.1038/nrm2866
- Ferris, S. H., and Farlow, M. (2013). Language impairment in Alzheimer's disease and benefits of acetylcholinesterase inhibitors. *Clin. Interv. Aging* 8, 1007–1014. doi: 10.2147/CIA.S39959
- French, C. A., Groszer, M., Preece, C., Coupe, A.-M., Rajewsky, K., and Fisher, S. E. (2007). Generation of mice with a conditional *Foxp2* null allele. *Genesis* 45, 440–446. doi: 10.1002/dvg.20305
- Geisen, M. J., Di Meglio, T., Pasqualetti, M., Ducret, S., Brunet, J.-F., Chedotal, A., et al. (2008). *Hox* paralogue group 2 genes control the migration of mouse pontine neurons through slit- robo signaling. *PLoS Biol.* 6:e142. doi: 10.1371/journal.pbio.0060142
- Georgantia, E.-M., Tsoutsis, L., Gaitanou, M., and Georgoussi, Z. (2013). δ -opioid receptor activation leads to neurite outgrowth and neuronal differentiation via a STAT5B-Gai/o pathway. *J. Neurochem.* 127, 329–341. doi: 10.1111/jnc.12386
- Georgescu, M.-M., Cote, G., Agarwal, N. K., and White, C. L. (2014). NHERF1/EBP50 controls morphogenesis of 3D colonic glands by stabilizing PTEN and ezrin-radixin-moesin proteins at the apical membrane. *Neoplasia* 16, 365–374.e2. doi: 10.1016/j.neo.2014.04.004
- Grati, M., Chakchouk, I., Ma, Q., Bensaïd, M., Desmidt, A., Turki, N., et al. (2015). A missense mutation in DCDC2 causes human recessive deafness DFNB66, likely by interfering with sensory hair cell and supporting cell cilia length regulation. *Hum. Mol. Genet.* 24, 2482–2491. doi: 10.1093/hmg/ddv009
- Haesler, S., Rochefort, C., Georgi, B., Licznarski, P., Osten, P., and Scharff, C. (2007). Incomplete and inaccurate vocal imitation after knockdown of *FoxP2* in songbird basal ganglia nucleus Area X. *PLoS Biol.* 5:e321. doi: 10.1371/journal.pbio.0050321
- Haesler, S., Wada, K., Nshdejan, A., Morrisey, E. E., Lints, T., Jarvis, E. D., et al. (2004). *FoxP2* expression in avian vocal learners and non-learners. *J. Neurosci.* 24, 3164–3175. doi: 10.1523/JNEUROSCI.4369-03.2004
- Hall, T. A. (1999). BioEdit: a user-friendly biological sequence alignment editor and analysis program for Windows 95/98/NT. *Nucl. Acids Symp. Ser.* 41, 95–98.
- Han, B.-S., Iacovitti, L., Katano, T., Hattori, N., Seol, W., and Kim, K.-S. (2008). Expression of the LRRK2 gene in the midbrain dopaminergic neurons of the substantia nigra. *Neurosci. Lett.* 442, 190–194. doi: 10.1016/j.neulet.2008.06.086
- Hayashi, T., Rizzuto, R., Hajnoczky, G., and Su, T.-P. (2009). MAM: more than just a housekeeper. *Trends Cell Biol.* 19, 81–88. doi: 10.1016/j.tcb.2008.12.002
- Hertel, N., and Redies, C. (2011). Absence of layer-specific cadherin expression profiles in the neocortex of the reeler mutant mouse. *Cereb. Cortex* 21, 1105–1117. doi: 10.1093/cercor/bhq183
- Higo, T., Hattori, M., Nakamura, T., Natsume, T., Michikawa, T., and Mikoshiba, K. (2005). Subtype-specific and ER lumenal environment-dependent regulation of inositol 1,4,5-trisphosphate receptor type 1 by ERp44. *Cell* 120, 85–98. doi: 10.1016/j.cell.2004.11.048
- Hilliard, A. T., Miller, J. E., Fraley, E. R., Horvath, S., and White, S. A. (2012). Molecular microcircuitry underlies functional specification in a basal ganglia circuit dedicated to vocal learning. *Neuron* 73, 537–552. doi: 10.1016/j.neuron.2012.01.005
- Hirsch, M.-R., d'Autreaux, F., Dymecki, S. M., Brunet, J.-F., and Goridis, C. (2013). A Phox2b:FLPo transgenic mouse line suitable for intersectional genetics. *Genesis* 51, 506–514. doi: 10.1002/dvg.22393
- Ismail, A., Ning, K., Al-Hayani, A., Sharrack, B., and Azzouz, M. (2012). *PTEN*: a molecular target for neurodegenerative disorders. *Transl. Neurosci.* 3, 132–142. doi: 10.2478/s13380-012-0018-9
- Jamadar, S., Powers, N. R., Meda, S. A., Gelernter, J., Gruen, J. R., and Pearson, G. D. (2011). Genetic influences of cortical gray matter in language-related regions in healthy controls and schizophrenia. *Schizophr. Res.* 129, 141–148. doi: 10.1016/j.schres.2011.03.027
- Jiang, H., and Wong, W. H. (2008). SeqMap: mapping massive amount of oligonucleotides to the genome. *Bioinformatics* 24, 2395–2396. doi: 10.1093/bioinformatics/btn429
- Kannan, M. B., Solovieva, V., and Blank, V. (2012). The small MAF transcription factors MAFF, MAFK and MAFK: current knowledge and perspectives. *Biochim. Biophys. Acta* 1823, 1841–1846. doi: 10.1016/j.bbamcr.2012.06.012
- Kato, M., Okanoya, K., Koike, T., Sasaki, E., Okano, H., Watanabe, S., et al. (2014). Human speech- and reading-related genes display partially overlapping expression patterns in the marmoset brain. *Brain Lang.* 133, 26–38. doi: 10.1016/j.bandl.2014.03.007
- Keller, C. A., Yuan, X., Panzanelli, P., Martin, M. L., Alldred, M., Sassoe-Pognetto, M., et al. (2004). The $\gamma 2$ subunit of GABA(A) receptors is a substrate for palmitoylation by GODZ. *J. Neurosci.* 24, 5881–5891. doi: 10.1523/JNEUROSCI.1037-04.2004
- Kerin, T., Ramanathan, A., Rivas, K., Grepo, N., Coetzee, G. A., and Campbell, D. B. (2012). A noncoding RNA antisense to moesin at 5p14.1 in autism. *Sci. Transl. Med.* 4:128ra40. doi: 10.1126/scitranslmed.3003479
- Kim, C.-H., Han, B.-S., Moon, J., Kim, D.-J., Shin, J., Rajan, S., et al. (2015). Nuclear receptor Nurr1 agonists enhance its dual functions and improve behavioral deficits in an animal model of Parkinson's disease. *Proc. Natl. Acad. Sci. U.S.A.* 112, 8756–8761. doi: 10.1073/pnas.1509742112
- Kimura, Y., Matsunami, H., Inoue, T., Shimamura, K., Uchida, N., Ueno, T., et al. (1995). Cadherin-11 expressed in association with mesenchymal morphogenesis in the head, somite, and limb bud of early mouse embryos. *Dev. Biol.* 169, 347–358. doi: 10.1006/dbio.1995.1149
- King, M. C., and Wilson, A. C. (1975). Evolution at two levels in humans and chimpanzees. *Science* 188, 107–116. doi: 10.1126/science.1090005

- Ko, J., Fuccillo, M. V., Malenka, R. C., and Sudhof, T. C. (2009). LRRTM2 functions as a neuroligin ligand in promoting excitatory synapse formation. *Neuron* 64, 791–798. doi: 10.1016/j.neuron.2009.12.012
- Konopka, G., Bomar, J. M., Winden, K., Coppola, G., Jonsson, Z. O., Gao, F., et al. (2009). Human-specific transcriptional regulation of CNS development genes by FOXP2. *Nature* 462, 213–217. doi: 10.1038/nature08549
- Kupferberg, G. (2010). Language in schizophrenia part 1: an introduction. *Lang. Linguist. Compass.* 4, 576–589. doi: 10.1111/j.1749-818X.2010.00216.x
- Lee, H.-C., Tan, K.-L., Cheah, P.-S., and Ling, K.-H. (2016). Potential role of JAK-STAT signaling pathway in the neurogenic-to-gliogenic shift in Down syndrome brain. *Neural Plast.* 2016:7434191. doi: 10.1155/2016/7434191
- Leslie, J. R., Imai, F., Fukuhara, K., Takegahara, N., Rizvi, T. A., Friedel, R. H., et al. (2011). Ectopic myelinating oligodendrocytes in the dorsal spinal cord as a consequence of altered semaphorin 6D signaling inhibit synapse formation. *Development* 138, 4085–4095. doi: 10.1242/dev.066076
- Li, T., Zeng, Z., Zhao, Q., Wang, T., Huang, K., Li, J., et al. (2013). *FoxP2* is significantly associated with schizophrenia and major depression in the Chinese Han population. *World J. Biol. Psychiatry* 14, 146–150. doi: 10.3109/15622975.2011.615860
- Livak, K. J., and Schmittgen, T. D. (2001). Analysis of relative gene expression data using real-time quantitative PCR and the 2⁻(Delta Delta C(T)) Method. *Methods* 25, 402–408. doi: 10.1006/meth.2001.1262
- Lubec, B., Weitzdoerfer, R., and Fountoulakis, M. (2001). Manifold reduction of moesin in fetal Down syndrome brain. *Biochem. Biophys. Res. Commun.* 286, 1191–1194. doi: 10.1006/bbrc.2001.5520
- Mallick, S., Li, H., Lipson, M., Mathieson, I., Gymrek, M., Racimo, F., et al. (2016). The simons genome diversity project: 300 genomes from 142 diverse populations. *Nature* 538, 201–206. doi: 10.1038/nature18964
- Marcus, G. F., and Fisher, S. E. (2003). FOXP2 in focus: what can genes tell us about speech and language? *Trends Cogn. Sci.* 7, 257–262. doi: 10.1016/S1364-6613(03)00104-9
- Matsunaga, E., Nambu, S., Oka, M., and Iriki, A. (2015). Complex and dynamic expression of cadherins in the embryonic marmoset cerebral cortex. *Dev. Growth Differ.* 57, 474–483. doi: 10.1111/dgd.12228
- Matsunami, H., Miyatani, S., Inoue, T., Copeland, N. G., Gilbert, D. J., Jenkins, N. A., et al. (1993). Cell binding specificity of mouse R-cadherin and chromosomal mapping of the gene. *J. Cell Sci.* 106, 401–409.
- McMahon, M., Campbell, K. H., MacLeod, A. K., McLaughlin, L. A., Henderson, C. J., and Wolf, C. R. (2014). HDAC inhibitors increase NRF2-signaling in tumour cells and blunt the efficacy of co-administered cytotoxic agents. *PLoS ONE* 9:e114055. doi: 10.1371/journal.pone.0114055
- Meng, H., Smith, S. D., Hager, K., Held, M., Liu, J., Olson, R. K., et al. (2005). *DCDC2* is associated with reading disability and modulates neuronal development in the brain. *Proc. Natl. Acad. Sci. U.S.A.* 102, 17053–17058. doi: 10.1073/pnas.0508591102
- Miller, C., Saada, A., Shaul, N., Shabtai, N., Ben-Shalom, E., Shaag, A., et al. (2004). Defective mitochondrial translation caused by a ribosomal protein (MRPS16) mutation. *Ann. Neurol.* 56, 734–738. doi: 10.1002/ana.20282
- Mitin, N., Ramocki, M. B., Konieczny, S. F., and Taparowsky, E. J. (2001). “Ras regulation of skeletal muscle differentiation and gene expression,” in *Methods in Enzymology, Regulators and Effectors of Small GTPases*, Vol. 333, eds W. E. Balch and C. J. Der (New York: Springer), 232–246.
- Monticelli, S., and Rao, A. (2002). NFAT1 and NFAT2 are positive regulators of IL-4 gene transcription. *Eur. J. Immunol.* 32, 2971–2978. doi: 10.1002/1521-4141(200210)32:10<2971::AID-IMMU2971>3.0.CO;2-G
- Mori, S., Maher, P., and Conti, B. (2016). Neuroimmunology of the interleukins 13 and 4. *Brain Sci.* 6, E18. doi: 10.3390/brainsci6020018
- Morrison, B. E., Marcondes, M. C. G., Nomura, D. K., Sanchez-Alavez, M., Sanchez-Gonzalez, A., Saar, I., et al. (2012). Cutting edge: IL-13Ralpha1 expression in dopaminergic neurons contributes to their oxidative stress-mediated loss following chronic peripheral treatment with lipopolysaccharide. *J. Immunol.* 189, 5498–5502. doi: 10.4049/jimmunol.1102150
- Mortazavi, A., Williams, B. A., McCue, K., Schaeffer, L., and Wold, B. (2008). Mapping and quantifying mammalian transcriptomes by RNA-Seq. *Nat. Methods* 5, 621–628. doi: 10.1038/nmeth.1226
- Mozzi, A., Forni, D., Clerici, M., Pozzoli, U., Mascheretti, S., Guerini, F. R., et al. (2016). The evolutionary history of genes involved in spoken and written language: beyond FOXP2. *Sci. Rep.* 6:22157. doi: 10.1038/srep22157
- Murray, L. L. (2000). Spoken language production in Huntington’s and Parkinson’s diseases. *J. Speech Lang. Hear. Res.* 43, 1350–1366. doi: 10.1044/jslhr.4306.1350
- Mylykangas, L., Wavrant-De Vrieze, F., Polvikoski, T., Notkola, I.-L., Sulkava, R., Niinisto, L., et al. (2005). Chromosome 21 *BACE2* haplotype associates with Alzheimer’s disease: a two-stage study. *J. Neurol. Sci.* 236, 17–24. doi: 10.1016/j.jns.2005.04.008
- Nakada, C., Satoh, S., Tabata, Y., Arai, K.-I., and Watanabe, S. (2006). Transcriptional repressor foxl1 regulates central nervous system development by suppressing shh expression in zebra fish. *Mol. Cell. Biol.* 26, 7246–7257. doi: 10.1128/MCB.00429-06
- Nayak, G. D., Ratnayaka, H. S., Goodyear, R. J., and Richardson, G. P. (2007). Development of the hair bundle and mechanotransduction. *Int. J. Dev. Biol.* 51, 597–608. doi: 10.1387/ijdb.072392gn
- Nelson, C. S., Fuller, C. K., Fordyce, P. M., Greninger, A. L., Li, H., and DeRisi, J. L. (2013). Microfluidic affinity and CHIP-seq analyses converge on a conserved FOXP2-binding motif in chimp and human, which enables the detection of evolutionarily novel targets. *Nucleic Acids Res.* 41, 5991–6004. doi: 10.1093/nar/gkt259
- Neves-Pereira, M., Muller, B., Massie, D., Williams, J. H. G., O’Brien, P. C. M., Hughes, A., et al. (2009). Deregulation of EIF4E: a novel mechanism for autism. *J. Med. Genet.* 46, 759–765. doi: 10.1136/jmg.2009.066852
- Newbury, D. F., Paracchini, S., Scerri, T. S., Winchester, L., Addis, L., Richardson, A. J., et al. (2011). Investigation of dyslexia and SLI risk variants in reading- and language-impaired subjects. *Behav. Genet.* 41, 90–104. doi: 10.1007/s10519-010-9424-3
- Noseda, R., Guerrero-Valero, M., Alberizzi, V., Previtali, S. C., Sherman, D. L., Palmisano, M., et al. (2016). Kif13b regulates PNS and CNS myelination through the Dlg1 scaffold. *PLoS Biol.* 14:e1002440. doi: 10.1371/journal.pbio.1002440
- Oblander, S. A., and Brady-Kalnay, S. M. (2010). Distinct PTPmu-associated signaling molecules differentially regulate neurite outgrowth on E-, N-, and R-cadherin. *Mol. Cell. Neurosci.* 44, 78–93. doi: 10.1016/j.mcn.2010.02.005
- O’Brien, R. J., and Wong, P. C. (2011). Amyloid precursor protein processing and Alzheimer’s disease. *Annu. Rev. Neurosci.* 34, 185–204. doi: 10.1146/annurev-neuro-061010-113613
- Open Science Collaboration. (2012). An open, large-scale, collaborative effort to estimate the reproducibility of psychological science. *Perspect. Psychol. Sci.* 7, 657–660. doi: 10.1177/1745691612462588
- Oukhai, K., Maricic, N., Schneider, M., Harzer, W., and Tausche, E. (2011). Developmental myosin heavy chain mRNA in masseter after orthognathic surgery: a preliminary study. *J. Craniomaxillofac. Surg.* 39, 401–406. doi: 10.1016/j.jcms.2010.06.001
- Paisan-Ruiz, C., Nath, P., Washecka, N., Gibbs, J. R., and Singleton, A. B. (2008). Comprehensive analysis of LRRK2 in publicly available Parkinson’s disease cases and neurologically normal controls. *Hum. Mutat.* 29, 485–490. doi: 10.1002/humu.20668
- Palka, C., Alfonsi, M., Mohn, A., Cerbo, R., Guanciali Franchi, P., Fantasia, D., et al. (2012). Mosaic 7q31 deletion involving FOXP2 gene associated with language impairment. *Pediatrics* 129, e183–e188. doi: 10.1542/peds.2010-2094
- Pan, H. C., Yang, C. N., Hung, Y. W., Lee, W. J., Tien, H. R., Shen, C. C., et al. (2013). Reciprocal modulation of C/EBP- α and C/EBP- β by IL-13 in activated microglia prevents neuronal death. *Eur. J. Immunol.* 43, 2854–2865. doi: 10.1002/eji.201343301
- Papapetropoulos, S., Ffrench-Mullen, J., McCorquodale, D., Qin, Y., Pablo, J., and Mash, D. C. (2006). Multiregional gene expression profiling identifies MRPS6 as a possible candidate gene for Parkinson’s disease. *Gene Expr.* 13, 205–215. doi: 10.3727/000000006783991827
- Parisiadou, L., Xie, C., Cho, H. J., Lin, X., Gu, X.-L., Long, C.-X., et al. (2009). Phosphorylation of ezrin/radixin/moesin proteins by LRRK2 promotes the rearrangement of actin cytoskeleton in neuronal morphogenesis. *J. Neurosci.* 29, 13971–13980. doi: 10.1523/JNEUROSCI.3799-09.2009
- Paulson, A. F., Prasad, M. S., Thuringer, A. H., and Manzerra, P. (2014). Regulation of cadherin expression in nervous system development. *Cell Adh. Migr.* 8, 19–28. doi: 10.4161/cam.27839

- Perelman, P., Johnson, W. E., Roos, C., Seuánez, H. N., Horvath, J. E., Moreira, M. A. M., et al. (2011). A molecular phylogeny of living primates. *PLoS Genet.* 7:e1001342. doi: 10.1371/journal.pgen.1001342
- Périé, S., Agbulut, O., St Guily, J. L., and Butler-Browne, G. S. (2000). Myosin heavy chain expression in human laryngeal muscle fibers. A biochemical study. *Ann. Otol. Rhinol. Laryngol.* 109, 216–220. doi: 10.1177/000348940010900218
- Pfening, A. R., Hara, E., Whitney, O., Rivas, M. V., Wang, R., Roulhac, P. L., et al. (2014). Convergent transcriptional specializations in the brains of humans and song-learning birds. *Science* 346:1256846. doi: 10.1126/science.1256846
- Qin, H., Buckley, J. A., Li, X., Liu, Y., Fox, T. H., Meares, G. P., et al. (2016). Inhibition of the JAK/STAT pathway protects against α -synuclein-induced neuroinflammation and dopaminergic neurodegeneration. *J. Neurosci.* 36, 5144–5159. doi: 10.1523/JNEUROSCI.4658-15.2016
- Reilly, J., Rodriguez, A., Lamy, M., and Neils-Strunjas, J. (2010). Cognition, language, and clinical pathological features of non-Alzheimer's dementias: an overview. *J. Commun. Disord.* 43, 438–452. doi: 10.1016/j.jcomdis.2010.04.011
- Reimers-Kipping, S., Hevers, W., Pääbo, S., and Enard, W. (2011). Humanized *Foxp2* specifically affects cortico-basal ganglia circuits. *Neuroscience* 175, 75–84. doi: 10.1016/j.neuroscience.2010.11.042
- Roubinet, C., Decelle, B., Chicanne, G., Dorn, J. F., Payrastra, B., Payre, F., et al. (2011). Molecular networks linked by Moesin drive remodeling of the cell cortex during mitosis. *J. Cell Biol.* 195, 99–112. doi: 10.1083/jcb.201106048
- Roussio, D. L., Pearson, C. A., Gaber, Z. B., Miquelajaregui, A., Li, S., Portera-Cailliau, C., et al. (2012). Foxp-mediated suppression of N-cadherin regulates neuroepithelial character and progenitor maintenance in the CNS. *Neuron* 74, 314–330. doi: 10.1016/j.neuron.2012.02.024
- Sato, N., Yamamoto, T., Sekine, Y., Yumioka, T., Junicho, A., Fuse, H., et al. (2003). Involvement of heat-shock protein 90 in the interleukin-6-mediated signaling pathway through STAT3. *Biochem. Biophys. Res. Commun.* 300, 847–852. doi: 10.1016/S0006-291X(02)02941-8
- Schmunk, G., Boubion, B. J., Smith, I. F., Parker, I., and Gargus, J. J. (2015). Shared functional defect in IP(3)R-mediated calcium signaling in diverse monogenic autism syndromes. *Transl. Psychiatry* 5:e643. doi: 10.1038/tp.2015.123
- Schraders, M., Oostrik, J., Huygen, P. L. M., Strom, T. M., van Wijk, E., Kunst, H. P. M., et al. (2010). Mutations in *PTPRQ* are a cause of autosomal-recessive nonsyndromic hearing impairment DFNB84 and associated with vestibular dysfunction. *Am. J. Hum. Genet.* 86, 604–610. doi: 10.1016/j.ajhg.2010.02.015
- Schreiwis, C., Bornschein, U., Burguiere, E., Kerimoglu, C., Schreiter, S., Dannemann, M., et al. (2014). Humanized *Foxp2* accelerates learning by enhancing transitions from declarative to procedural performance. *Proc. Natl. Acad. Sci. U.S.A.* 111, 14253–14258. doi: 10.1073/pnas.1414542111
- Seki, Y.-I., Hayashi, K., Matsumoto, A., Seki, N., Tsukada, J., Ransom, J., et al. (2002). Expression of the suppressor of cytokine signaling-5 (SOCS5) negatively regulates IL-4-dependent STAT6 activation and Th2 differentiation. *Proc. Natl. Acad. Sci. U.S.A.* 99, 13003–13008. doi: 10.1073/pnas.202477099
- Shen, H., Zhu, H., Song, M., Tian, Y., Huang, Y., Zheng, H., et al. (2014). A selenosemicarbazone complex with copper efficiently down-regulates the 90-kDa heat shock protein HSP90AA1 and its client proteins in cancer cells. *BMC Cancer* 14:629. doi: 10.1186/1471-2407-14-629
- Spiteri, E., Konopka, G., Coppola, G., Bomar, J., Oldham, M., Ou, J., et al. (2007). Identification of the transcriptional targets of *FOXP2*, a gene linked to speech and language, in developing human brain. *Am. J. Hum. Genet.* 81, 1144–1157. doi: 10.1086/522237
- Stephane, M., Pellizzer, G., Fletcher, C. R., and McClannahan, K. (2007). Empirical evaluation of language disorder in schizophrenia. *J. Psychiatry. Neurosci.* 32, 250–258.
- Stroud, J. C., Wu, Y., Bates, D. L., Han, A., Nowick, K., Paabo, S., et al. (2006). Structure of the forkhead domain of *FOXP2* bound to DNA. *Structure* 14, 159–166. doi: 10.1016/j.str.2005.10.005
- Tanabe, Y., Fujiwara, Y., Matsuzaki, A., Fujita, E., Kasahara, T., Yuasa, S., et al. (2012). Temporal expression and mitochondrial localization of a *Foxp2* isoform lacking the forkhead domain in developing Purkinje cells. *J. Neurochem.* 122, 72–80. doi: 10.1111/j.1471-4159.2011.07524.x
- Tang, A. T., Campbell, W. B., and Nithipatikom, K. (2012). ROCK1 feedback regulation of the upstream small GTPase RhoA. *Cell. Signal.* 24, 1375–1380. doi: 10.1016/j.cellsig.2012.03.005
- Tilot, A. K., Bebek, G., Niazi, F., Altemus, J., Todd, R., Frazier, T. W., et al. (2016). Neural transcriptome of constitutional Pten dysfunction in mice and its relevance to human idiopathic Autism Spectrum Disorder. *Mol. Psychiatry* 21, 118–125. doi: 10.1038/mp.2015.17
- Tokita, M. J., Chow, P. M., Mirzaa, G., Dikow, N., Maas, B., Isidor, B., et al. (2015). Five children with deletions of 1p34.3 encompassing *AGO1* and *AGO3*. *Eur. J. Hum. Genet.* 23, 761–765. doi: 10.1038/ejhg.2014.202
- Toydemir, R. M., Chen, H., Proud, V. K., Martin, R., van Bokhoven, H., Hamel, B. C. J., et al. (2006). Trismus-pseudocamptodactyly syndrome is caused by recurrent mutation of *MYH8*. *Am. J. Med. Genet. A* 140, 2387–2393. doi: 10.1002/ajmg.a.31495
- Turner, S. J., Hildebrand, M. S., Block, S., Damiano, J., Fahey, M., Reilly, S., et al. (2013). Small intragenic deletion in *FOXP2* associated with childhood apraxia of speech and dysarthria. *Am. J. Med. Genet. A* 161A, 2321–2326. doi: 10.1002/ajmg.a.36055
- Tyzack, G. E., Sitnikov, S., Barson, D., Adams-Carr, K. L., Lau, N. K., Kwok, J. C., et al. (2014). Astrocyte response to motor neuron injury promotes structural synaptic plasticity via STAT3-regulated TSP-1 expression. *Nat. Commun.* 5:4294. doi: 10.1038/ncomms5294
- Uchida, N., Hoshino, S.-I., and Katada, T. (2004). Identification of a human cytoplasmic poly(A) nuclease complex stimulated by poly(A)-binding protein. *J. Biol. Chem.* 279, 1383–1391. doi: 10.1074/jbc.M309125200
- Velazquez, R., Shaw, D. M., Caccamo, A., and Oddo, S. (2016). Pim1 inhibition as a novel therapeutic strategy for Alzheimer's disease. *Mol. Neurodegener.* 11:52. doi: 10.1186/s13024-016-0118-z
- Vernes, S. C., and Fisher, S. E. (2009). Unravelling neurogenetic networks implicated in developmental language disorders. *Biochem. Soc. Trans.* 37, 1263–1269. doi: 10.1042/BST0371263
- Vernes, S. C., Newbury, D. F., Abrahams, B. S., Winchester, L., Nicod, J., Groszer, M., et al. (2008). A functional genetic link between distinct developmental language disorders. *N. Engl. J. Med.* 359, 2337–2345. doi: 10.1056/NEJMoa0802828
- Vernes, S. C., Nicod, J., Elahi, F. M., Coventry, J. A., Kenny, N., Coupe, A.-M., et al. (2006). Functional genetic analysis of mutations implicated in a human speech and language disorder. *Hum. Mol. Genet.* 15, 3154–3167. doi: 10.1093/hmg/ddl392
- Vernes, S. C., Oliver, P. L., Spiteri, E., Lockstone, H. E., Puliyadi, R., Taylor, J. M., et al. (2011). *Foxp2* regulates gene networks implicated in neurite outgrowth in the developing brain. *PLoS Genet.* 7:e1002145. doi: 10.1371/journal.pgen.1002145
- Vernes, S. C., Spiteri, E., Nicod, J., Groszer, M., Taylor, J. M., Davies, K. E., et al. (2007). High-throughput analysis of promoter occupancy reveals direct neural targets of *FOXP2*, a gene mutated in speech and language disorders. *Am. J. Hum. Genet.* 81, 1232–1250. doi: 10.1086/522238
- Walsh, J. T., Hendrix, S., Boato, F., Smirnov, I., Zheng, J., Lukens, J. R., et al. (2015). MHCII-independent CD4+ T cells protect injured CNS neurons via IL-4. *J. Clin. Invest.* 125, 699–714. doi: 10.1172/JCI76210
- Wang, K.-S., Zhang, Q., Liu, X., Wu, L., and Zeng, M. (2012). *PKNOX2* is associated with formal thought disorder in schizophrenia: a meta-analysis of two genome-wide association studies. *J. Mol. Neurosci.* 48, 265–272. doi: 10.1007/s12031-012-9787-4
- Weyler, R. T., Yurko-Mauro, K. A., Rubenstein, R., Kollen, W. J., Reenstra, W., Altschuler, S. M., et al. (1999). CFTR is functionally active in GnRH-expressing GT1-7 hypothalamic neurons. *Am. J. Physiol.* 277, C563–C571.
- Whiting, P. J., Bonner, T. P., McKernan, R. M., Farrar, S., Le Bourdelles, B., Heavens, R. P., et al. (1999). Molecular and functional diversity of the expanding GABA-A receptor gene family. *Ann. N. Y. Acad. Sci.* 868, 645–653. doi: 10.1111/j.1749-6632.1999.tb11341.x
- Wohlgenuth, S. E., Gorochowski, T. E., and Roubos, J. A. (2013). Translational sensitivity of the *Escherichia coli* genome to fluctuating tRNA availability. *Nucleic Acids Res.* 41, 8021–8033. doi: 10.1093/nar/gkt602
- Wolf, J. B. W., Kunstner, A., Nam, K., Jakobsson, M., and Ellegren, H. (2009). Nonlinear dynamics of nonsynonymous (dN) and synonymous (dS)

- substitution rates affects inference of selection. *Genome Biol. Evol.* 1, 308–319. doi: 10.1093/gbe/evp030
- Xiao, Q., Yang, S., and Le, W. (2015). G2019S LRRK2 and aging confer susceptibility to proteasome inhibitor-induced neurotoxicity in nigrostriatal dopaminergic system. *J. Neural. Transm. (Vienna)* 122, 1645–1657. doi: 10.1007/s00702-015-1438-9
- Yamazaki, H., Tanji, K., Wakabayashi, K., Matsuura, S., and Itoh, K. (2015). Role of the Keap1/Nrf2 pathway in neurodegenerative diseases. *Pathol. Int.* 65, 210–219. doi: 10.1111/pin.12261
- Yang, Z. (2007). PAML 4: a program package for phylogenetic analysis by maximum likelihood. *Mol. Biol. Evol.* 24, 1586–1591. doi: 10.1093/molbev/mst179
- Yoder, P. J., and Warren, S. F. (2004). Early predictors of language in children with and without Down syndrome. *Am. J. Ment. Retard.* 109, 285–300. doi: 10.1352/0895-8017
- Yoshimura, Y., Terabayashi, T., and Miki, H. (2010). Par1b/MARK2 phosphorylates kinesin-like motor protein GAKIN/KIF13B to regulate axon formation. *Mol. Cell. Biol.* 30, 2206–2219. doi: 10.1128/MCB.01181-09
- Zeng, F., Tian, Y., Shi, S., Wu, Q., Liu, S., Zheng, H., et al. (2011). Identification of mouse MARVELD1 as a microtubule associated protein that inhibits cell cycle progression and migration. *Mol. Cells* 31, 267–274. doi: 10.1007/s10059-011-0037-3
- Zetterström, R. H., Solomin, L., Jansson, L., Hoffer, B. J., Olson, L., and Perlmann, T. (1997). Dopamine neuron agenesis in Nurr1-deficient mice. *Science* 276, 248–250. doi: 10.1126/science.276.5310.248
- Zhang, J., Webb, D. M., and Podlaha, O. (2002). Accelerated protein evolution and origins of human-specific features: Foxp2 as an example. *Genetics* 162, 1825–1835.
- Zhao, G., Liu, Z., Ilagan, M. X. G., and Kopan, R. (2010). γ -secretase composed of PS1/Pen2/Aph1a can cleave notch and amyloid precursor protein in the absence of nicastrin. *J. Neurosci.* 30, 1648–1656. doi: 10.1523/JNEUROSCI.3826-09.2010
- Zhao, Y., Liu, X., Sun, H., Wang, Y., Yang, W., and Ma, H. (2015). Contactin-associated proteinlike 2 expression in SHSY5Y cells is upregulated by a FOXP2 mutant with a shortened polyglutamine tract. *Mol. Med. Rep.* 12, 8162–8168. doi: 10.3892/mmr.2015.4483
- Zheng, K., Heydari, B., and Simon, D. K. (2003). A common NURR1 polymorphism associated with Parkinson disease and diffuse Lewy body disease. *Arch. Neurol.* 60, 722–725. doi: 10.1001/archneur.60.5.722

Conflict of Interest Statement: The authors declare that the research was conducted in the absence of any commercial or financial relationships that could be construed as a potential conflict of interest.

Copyright © 2017 Oswald, Klöble, Ruland, Rosenkranz, Hinz, Butter, Ramljak, Zechner and Herlyn. This is an open-access article distributed under the terms of the Creative Commons Attribution License (CC BY). The use, distribution or reproduction in other forums is permitted, provided the original author(s) or licensor are credited and that the original publication in this journal is cited, in accordance with accepted academic practice. No use, distribution or reproduction is permitted which does not comply with these terms.